Lunar Section
BAA
British Astronomical Association
Director: Bill Leatherbarrow

LUNAR SECTION CIRCULAR

Vol. 57 No. 2 February 2020

FROM THE DIRECTOR

Dr Ron Maddison (January 1, 1935 – December 29, 2019)

Ron Maddison (right) and the Director, Keele University, 2012

It is with the deepest sadness that I report the death of Dr Ron Maddison on 29 December 2019. Ron served as Director of the Lunar Section from 1968 until 1971 and was responsible for steering the Section successfully through the years following the first Moon landings. He tailored the observing programme to ensure that it remained relevant in the post-Apollo era. At Keele University, where he worked as a Senior Lecturer in Physics, he was instrumental in the establishment of the University Observatory. He moved to Florida in 1991.

A fuller appreciation of Ron and his achievements will appear in due course, but in the meantime I am sure that Section members will wish to join me in extending our condolences to Ron's family.

Bill Leatherbarrow

Ron Maddison and Patrick Moore in 1975

OBSERVATIONS RECEIVED

Images have been received this month from the following observers: David Arditti, Clyde Foster (South Africa), Rik Hill (USA), Rod Lyon, Phil Masding, K C Pau (Hong Kong), Mark Radice, Dave Scanlan, and the Director.

PENUMBRAL LUNAR ECLIPSE, 10 January 2020

In addition, images and reports of the penumbral lunar eclipse of 10 January 2020 were received from: Gianluigi Adamoli (Italy), John Bracegirdle, Dave Eagle, Mike Foulkes, Mary McIntyre, Trevor Smith, Alexander Vandenbohede (Belgium), and Alex Vincent. Adamoli had particularly good conditions in Verona and used his 8x30 binoculars to provide a detailed report and timings of the progress of the eclipse. Many members' images have been posted on the observers' pages of the BAA website. Alex Vincent submitted a series of images showing the progress of the eclipse.

Maximum penumbral eclipse, 10 January 2020 (image by Dave Eagle, taken with a 190 Mak-Newt, D750 DSLR)

Alexander Vandenbohede used the WinJupos software to produce polar projections showing the penumbral shadow particularly well.

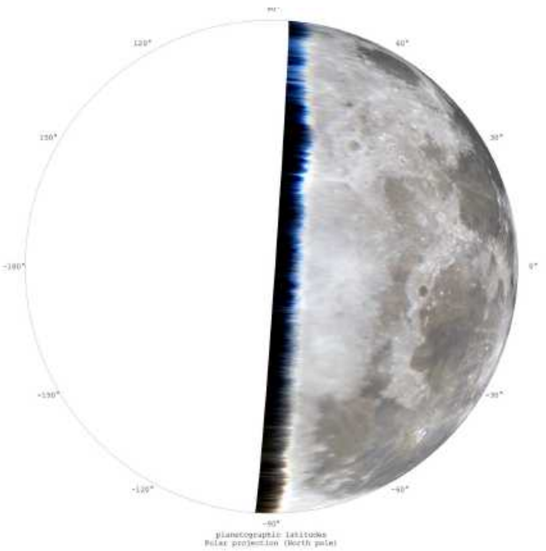

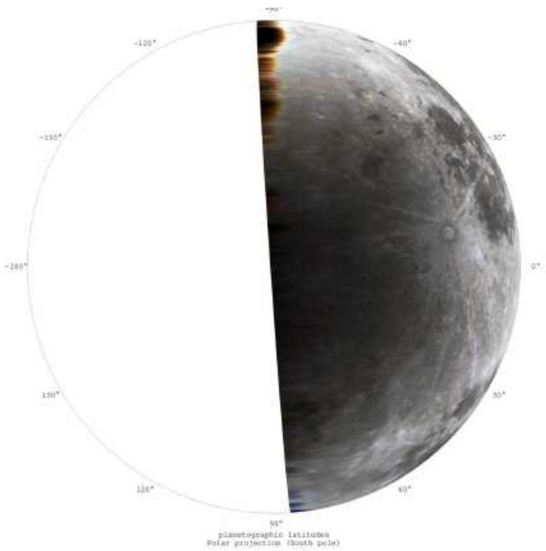

IMAGES GALLERY

Gruithuisen domes, 6 January 2020, 250mm SCT (Phil Masding)

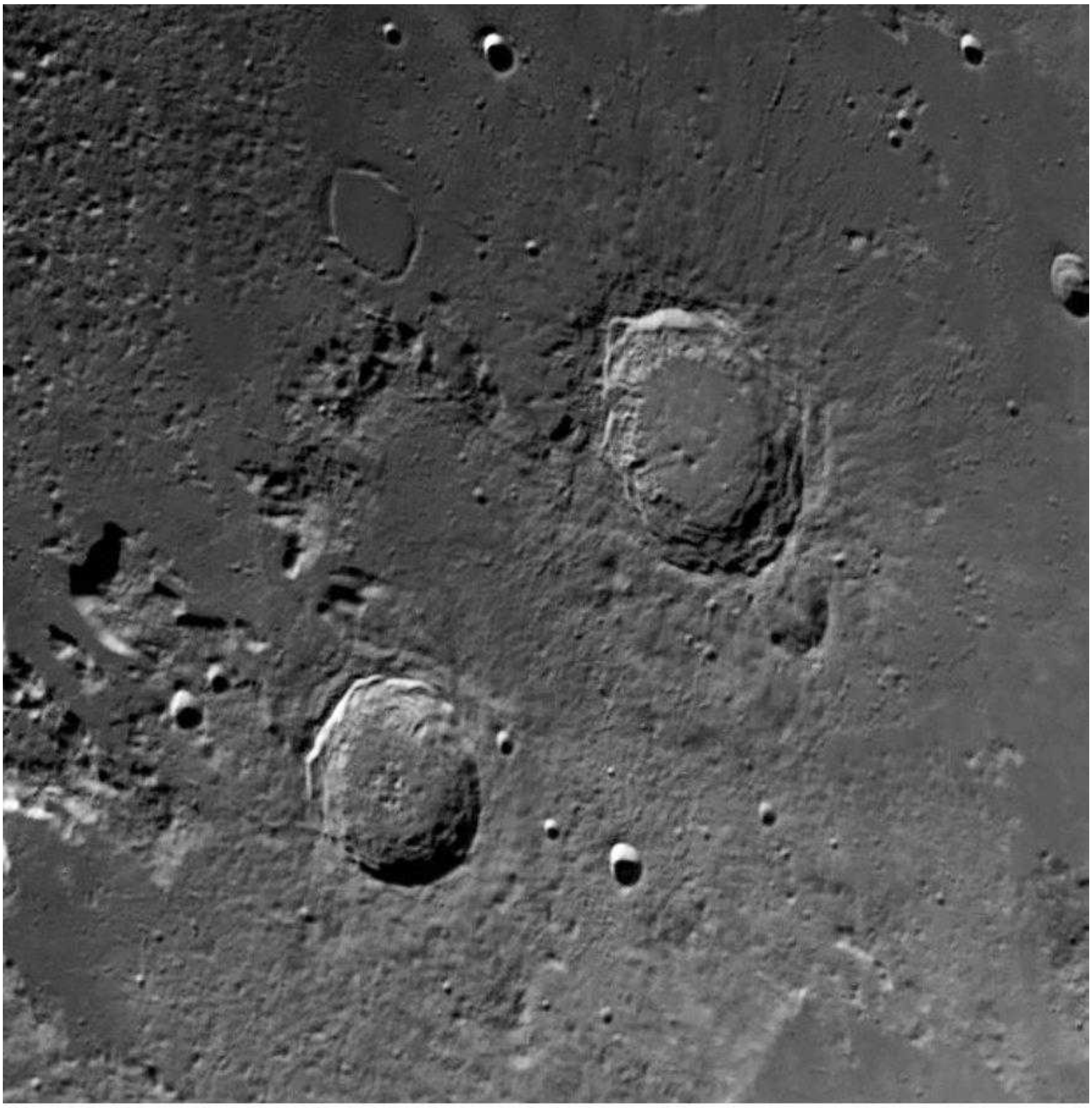

Aristoteles & Eudoxus 2020.01.03 - 17.53 UT
300mm Meade LX90, ASI 224MC Camera, with Pro Planet 742nm I-R Pass Filter. 1,000/5,000 Frames.
Seeing: 7/10

(image by Rod Lyon)

KC Pau has sent in two excellent images taken from his balcony in Hong Kong. He writes as follows:

‘Enclosed are two moon images taken in 2020. A wonderful start in a new year. The first photos is the panoramic view of Mare Serenitatis. This photo is taken on 02 Jan 2020 at 09h53m UT with my 10" f/6 Newtonian reflector, prime focus, QHYCCD290M and 450 frames stacked. I took this photo when the sky background was still very bright but the seeing was exceptionally steady. So many details are discerned and a little bit less contrasty when compared with photo taken in darker sky. The second photo was taken on 03 Jan 2020 at 12h05m UT with 10" f/6 Newtonian reflector + 20mm eyepiece projection + QHYCCD290M and 350 frames stacked. The photo shows the early sunrise over Montes Alpes. Gigantic shadows are thrown on the floor of Mare Imbrium. The tiny delicate rille is well-resolved in Vallis Alpes. One interesting view is the tips of the shadow of Mons Piton engulf a tiny crater.’

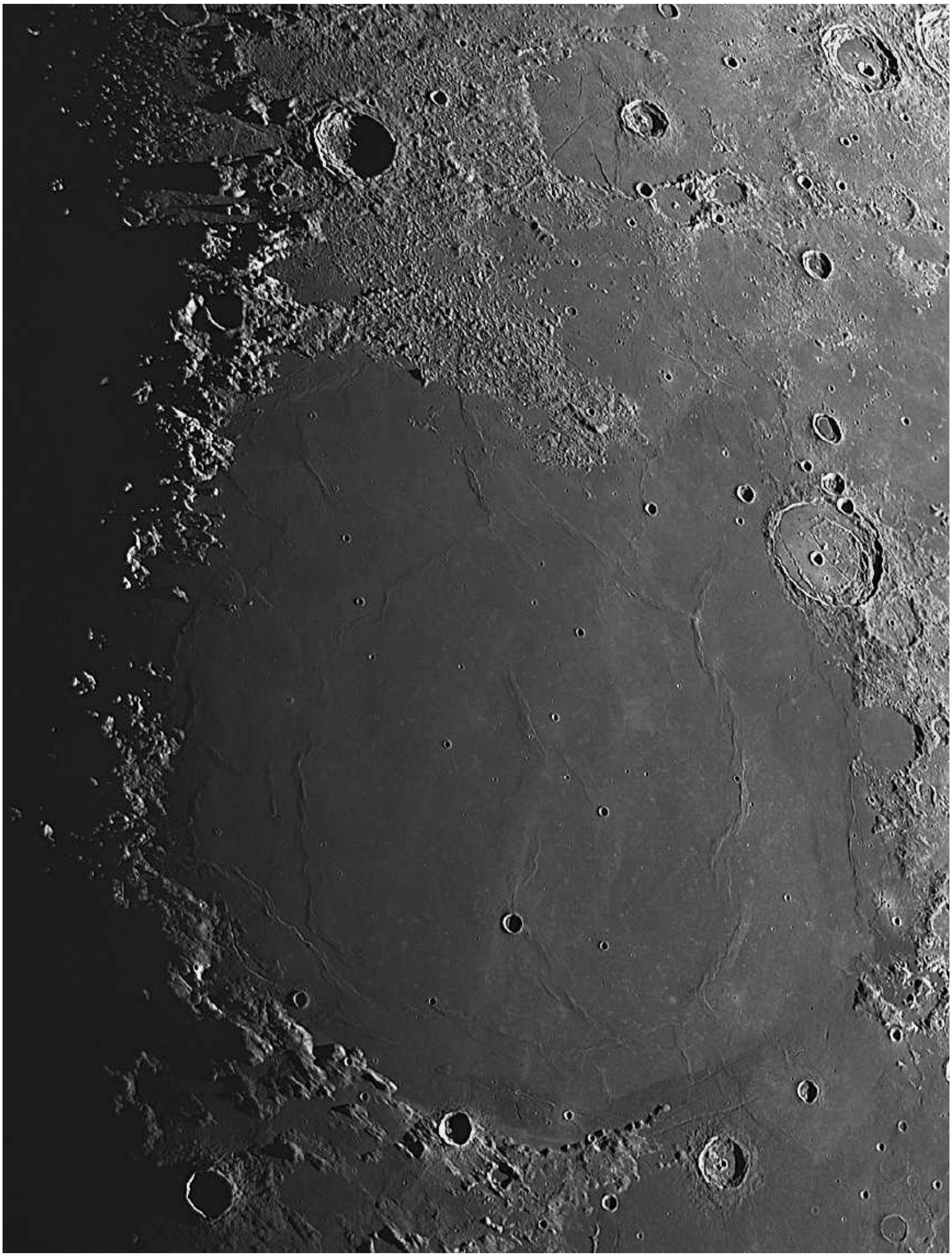

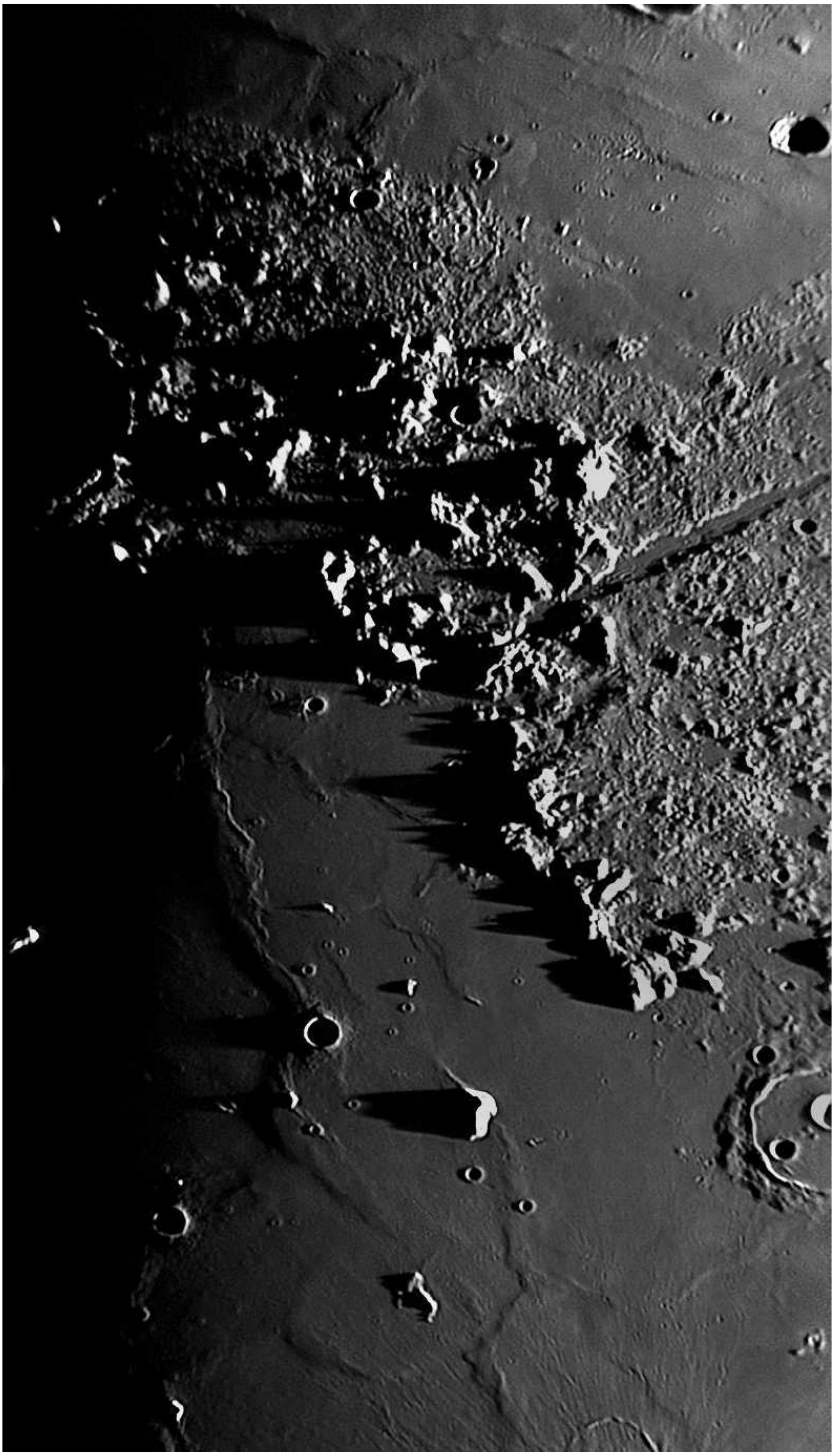

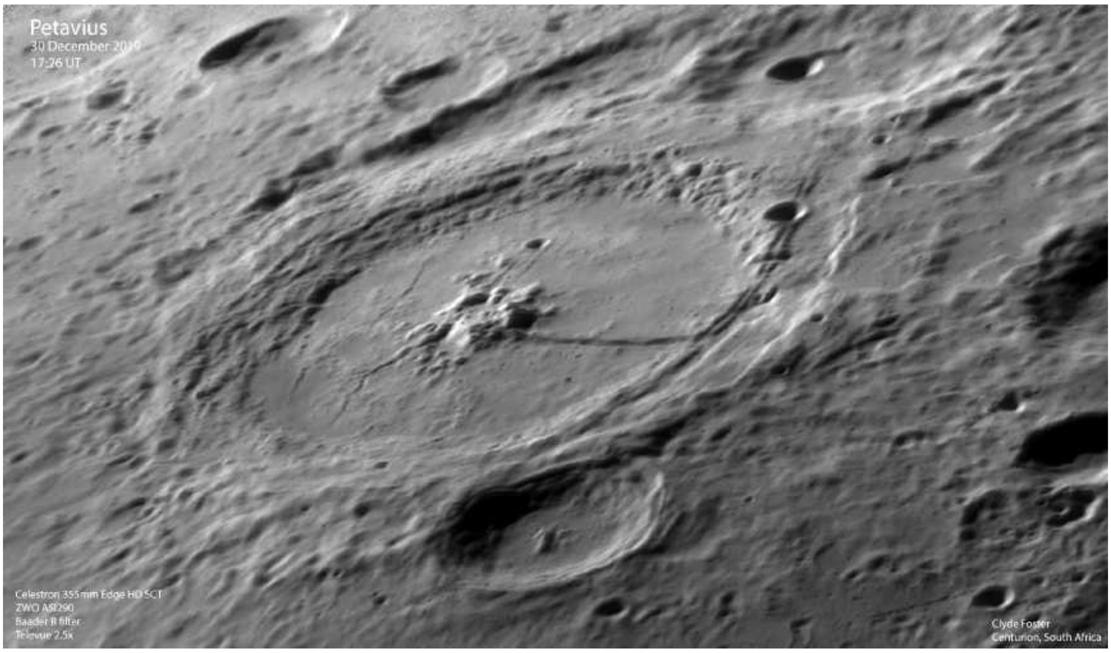

John Herschel, 6 January 2020, 22-18UT, OMC300 Mak-Cass (Bill Leatherbarrow)

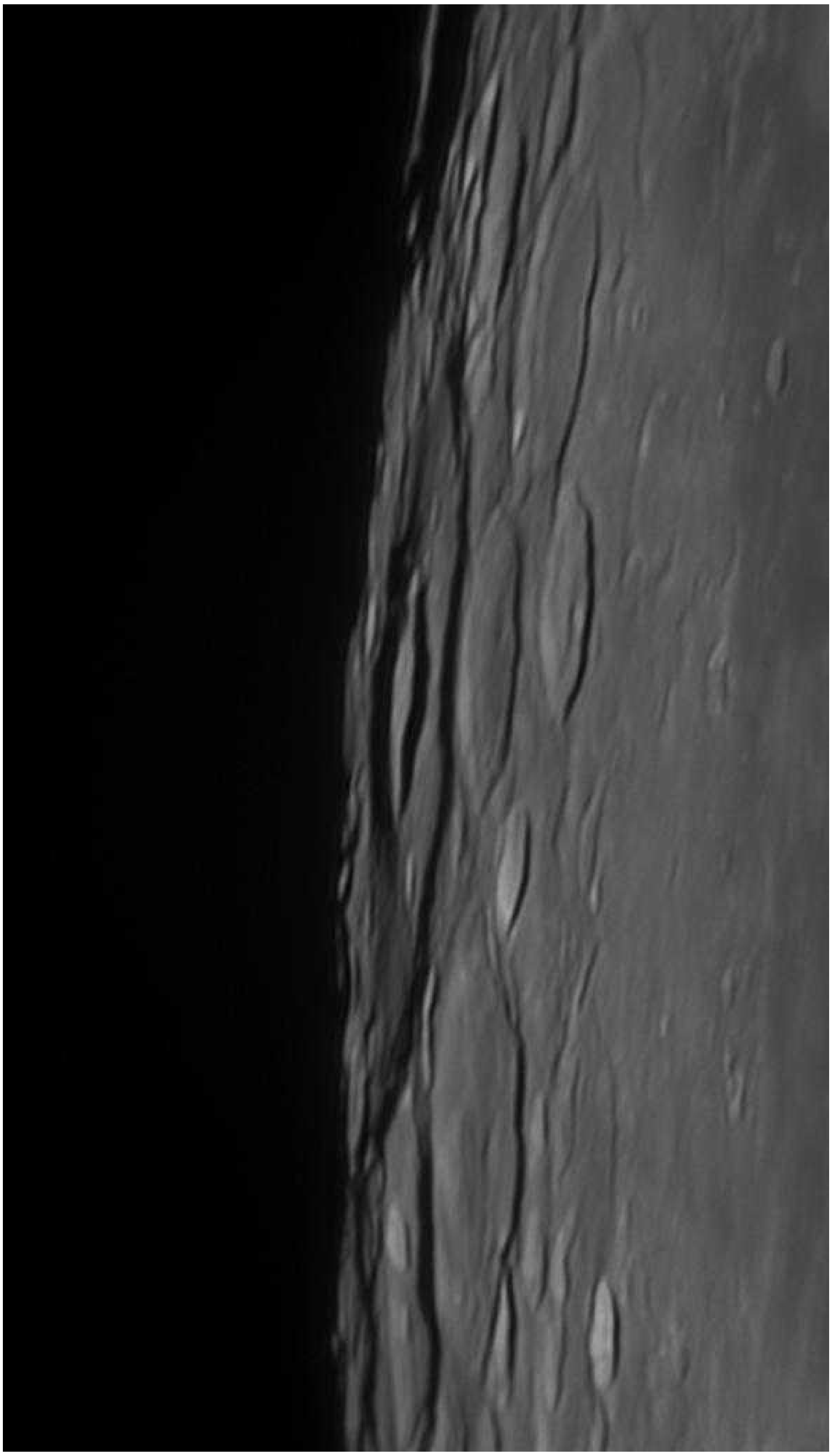

Einstein
11 December 2019 2053Z
C11 f20 ASI224MC 685nm IR filter
Mark Radice RefreshingViews.com

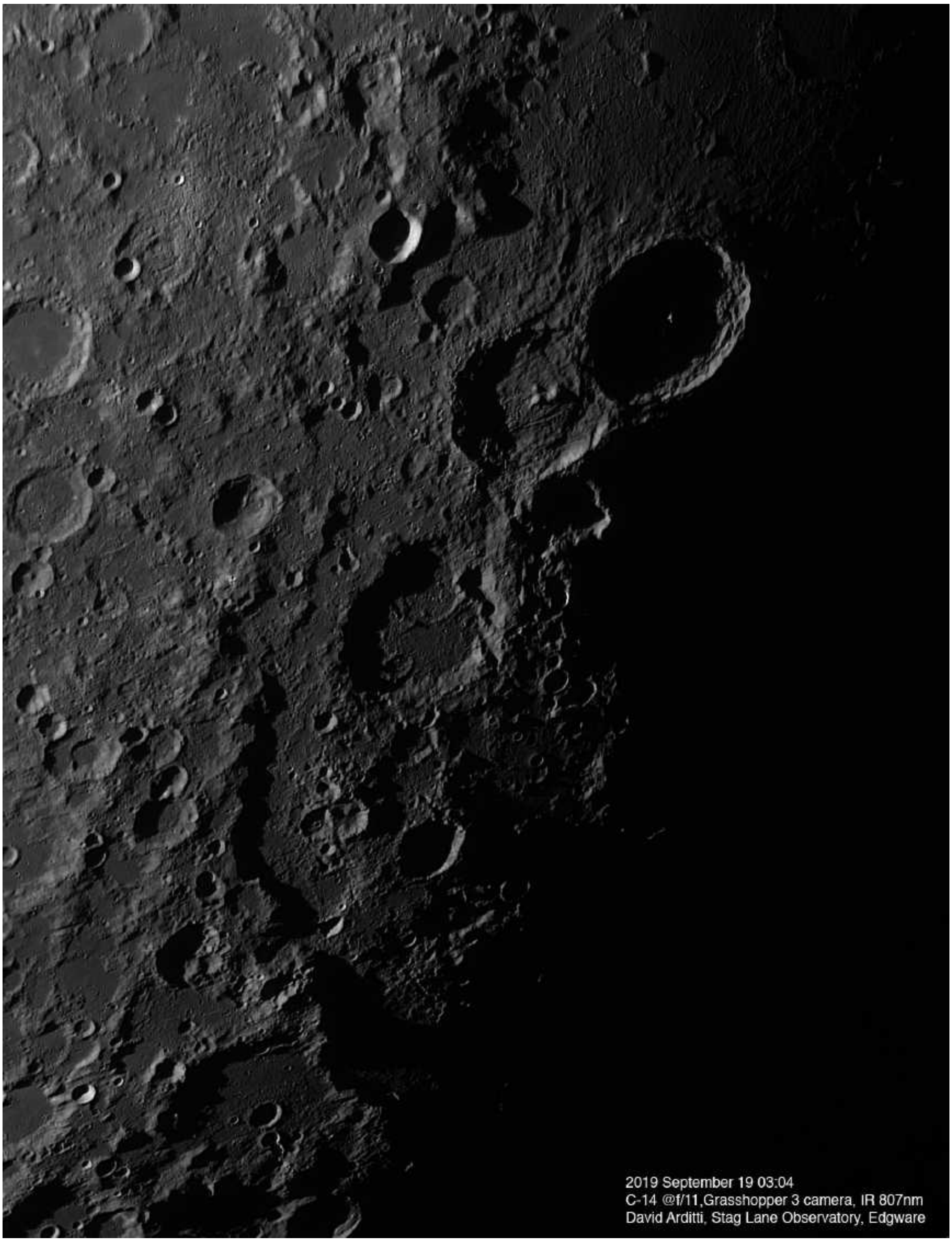

Theophilus-Cyrillus-Catharina trio

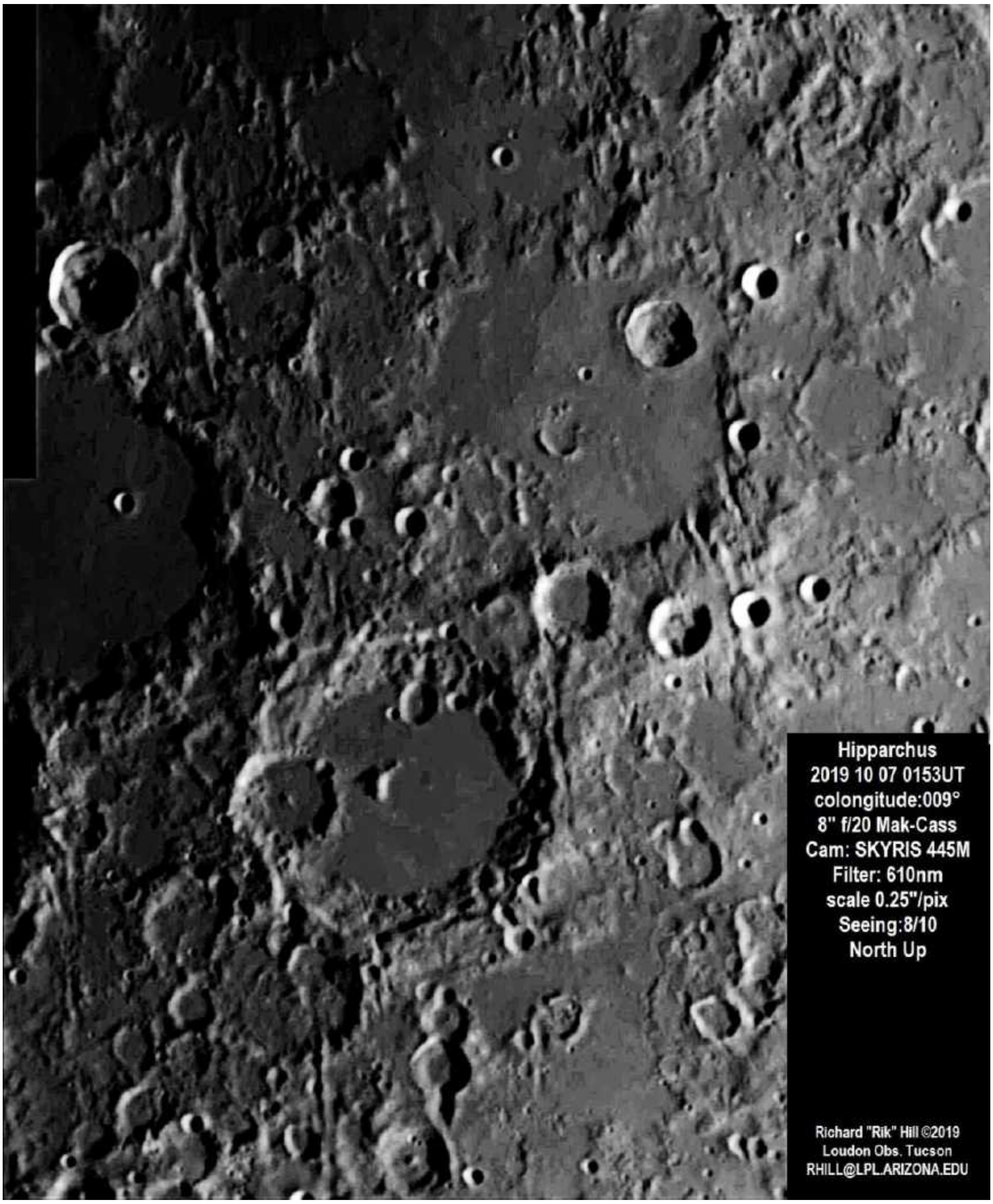

Rik Hill writes the following account of his image above:

‘There are two craters near the center of the visible disk of the Moon that would, in many other places, be highlights on their own but because of the proximity of spectacular craters they are lost in their glory. In this case half of the great crater Ptolemaeus can be seen on the left edge of this image and below it are, of course, Alphonsus and Arzachel all stealing the show. This overshadowing is just the case for Albategnius (82km diameter) and Hipparchus (155km). The former can be seen below and left of center in this image and the latter above center with the crisp, relatively recent Horrocks (31km) in the upper right, or northeast floor. Northeast of Horrocks is an even more recent crater, Pickering (15km) and due east of Horrocks is the remnants of a very ancient and hexagonal crater, Saunder (46km) possibly as old as 4.5 billion years!

Between the two main craters of this article is an interesting arc of four craters of decreasing diameter to the east. The first is Halley (37km) directly south of the center of Hipparchus followed to the east by Hind (31km) then Hipparchus-C (17km) and finally Hipparchus-L (12km). There is no significance to this configuration other than it makes a nice little eye catching grouping.

On the west wall of Albategnius is the crater Klein (46km) with a tiny central peak (most of it buried during the lava flooding event, and due east is the oddly shaped crater Ritchey (26km) its form the result of several merged impacts. Below Albategnius is an interesting group of features. The first are two craters with what looks to be a canyon cutting north-south through them. That canyon is actually a couple of small deformed craters on either end with your eye forming the rest of the canyon! This is easy to see in the LROC images. Below these is another nice crater, Argelander (36km) with a tiny central peak. Note the two sharply define tiny craters just above that central peak. These are very fresh, recent craters of 4km and 2.5km diameters. Before leaving, you should pay attention to the huge parallel scars all over this region. Just one of them was created by a city sized "rock" that was ejected as a secondary event during the Imbrium basin impact, in just a few seconds. Now imagine a whole fleet of them raking across the landscape plowing up phenomenal amount of soil and rock all in a few seconds! It must have been a terrible wonder to behold!!'

LUNAR DOMES (part XXXIV): A lunar dome near crater Prinz

Raffaello Lena and KC Pau

Prinz is the lava-flooded remains of a lunar impact crater on the Oceanus Procellarum. The formation lies to the northeast of the prominent crater Aristarchus. To the north-northeast is the flooded crater Krieger.

In this issue we examine a lunar dome near crater Prinz, located at latitude 24.39°N and longitude 41.64° W, of plausible intrusive origin.

The dome described in the current study (Fig. 1) was imaged by Pau on November 8, 2019 a 13:11 UT, using a Newtonian telescope of 250mm of diameter. The examined dome, imaged under a solar illumination angle of 3.8°, displays a flat shape (Fig. 1).

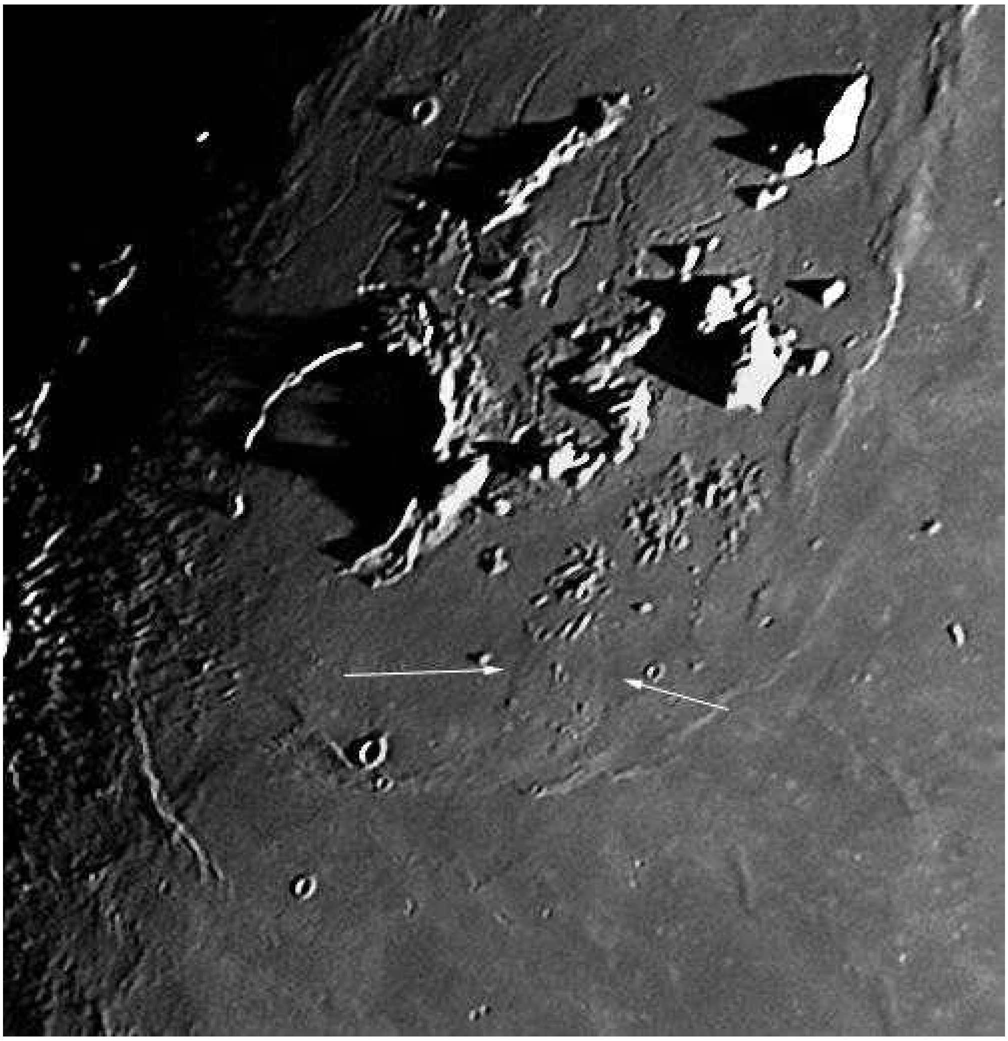

Figure 1: Prinz dome, termed Prinz 1, imaged by K.C. Pau on November 8, 2019, at 13:11 UT.

Intrusions are subsurface concentrations of magma that have locally uplifted the soil but do not erupt, a mechanism reported for terrestrial laccoliths [1].

A pressurised magma that penetrates between layers of solid rock may change the shape of these rocks, e.g. by bending them upwards, and solidifies without erupting to the surface. These magmatic processes are termed 'intrusive'. Laccoliths have been proposed to explain various geological features such as domes or floor-fractured craters on the surface of the Moon and also Mars and Mercury [2]. Terrestrial volcanic edifices may either form by an effusion of lava, e.g. resulting in shield volcanoes, or by an up-doming of rock layers caused by magma intrusion below the surface, resulting in intrusive domes [3-4].

Some lunar domes have smooth surfaces and very low cross-sectional profiles merging smoothly into the surrounding mare lava plains [5]. Some domes show fractures on their surfaces and are exceptionally large: they do not show summit pits and many of them are associated with faults or linear rilles of presumably tensional origin. As visible in Fig. 1 some prominences, non-volcanic hills, are situated on the summit of Prinz 1. The WAC image shows that the examined large dome displays linear rilles on its surface that can be interpreted as the result of tensional stress (Fig. 2): hence the flat dome is identified as an intrusive structure.

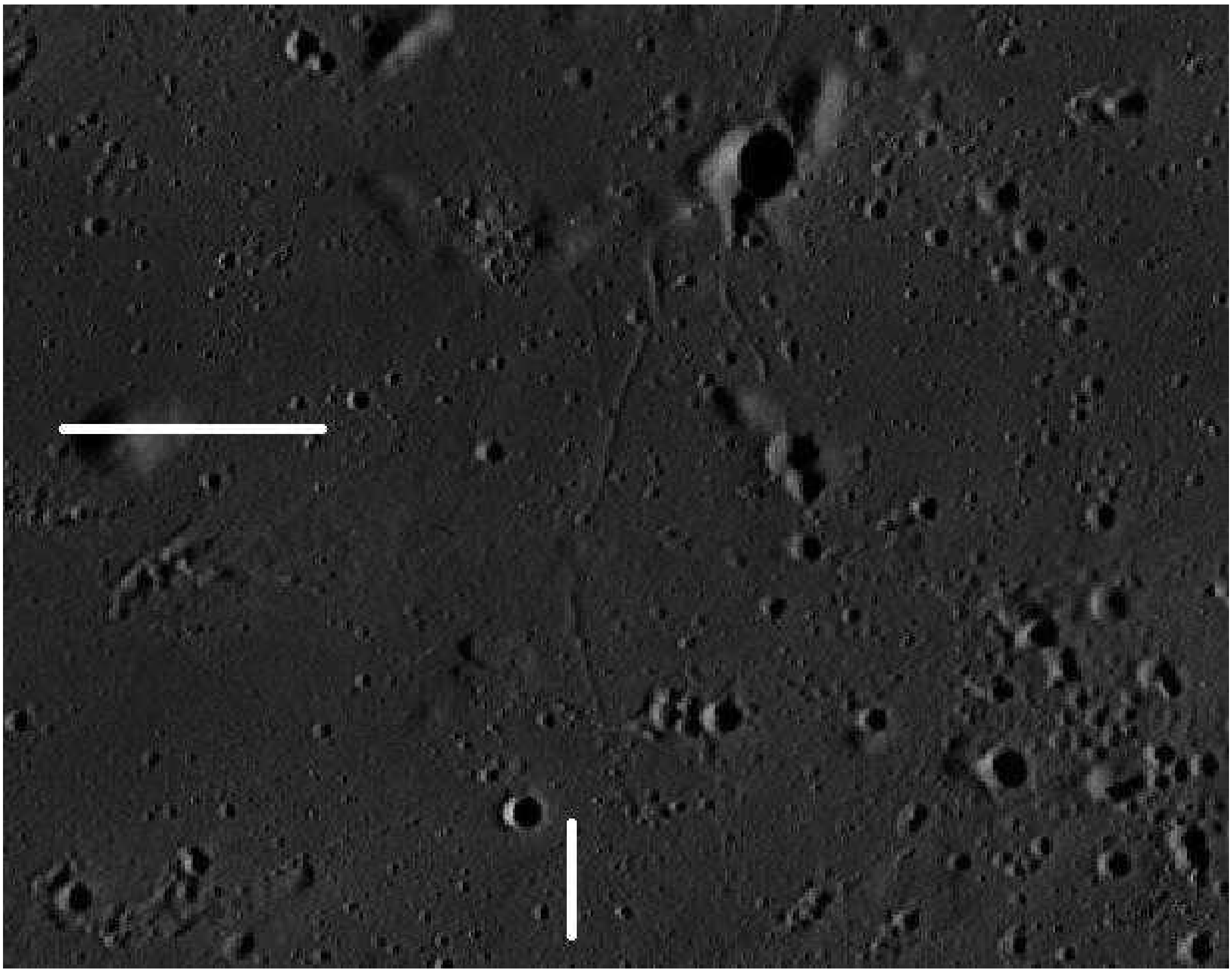

Figure 2: WAC imagery of Prinz 1 dome extracted from ACT react quick map in cylindrical projection.

Presumably, these hills are part of the underlying rugged basin floor below the mare lavas. The absence of a spectral contrast with the surrounding surface indicates that these structures are not a piece of pre-existing elevated terrain later embayed by basaltic lava, the so-called kipukas.

Based on LOLA DEM, the diameter is determined to 30 x 24 km. The height of Prinz 1 amounts to 60m ± 10m, resulting in an average slope of 0.3° ± 0.03°. The dome volume V is estimated by assuming a form factor of f = 1/2, which yields an edifice volume of 17km³.

ACT-REACT Quick Map tool is used to access to the LOLA DEM dataset, allowing us to obtain the cross-sectional profile (Fig. 3).

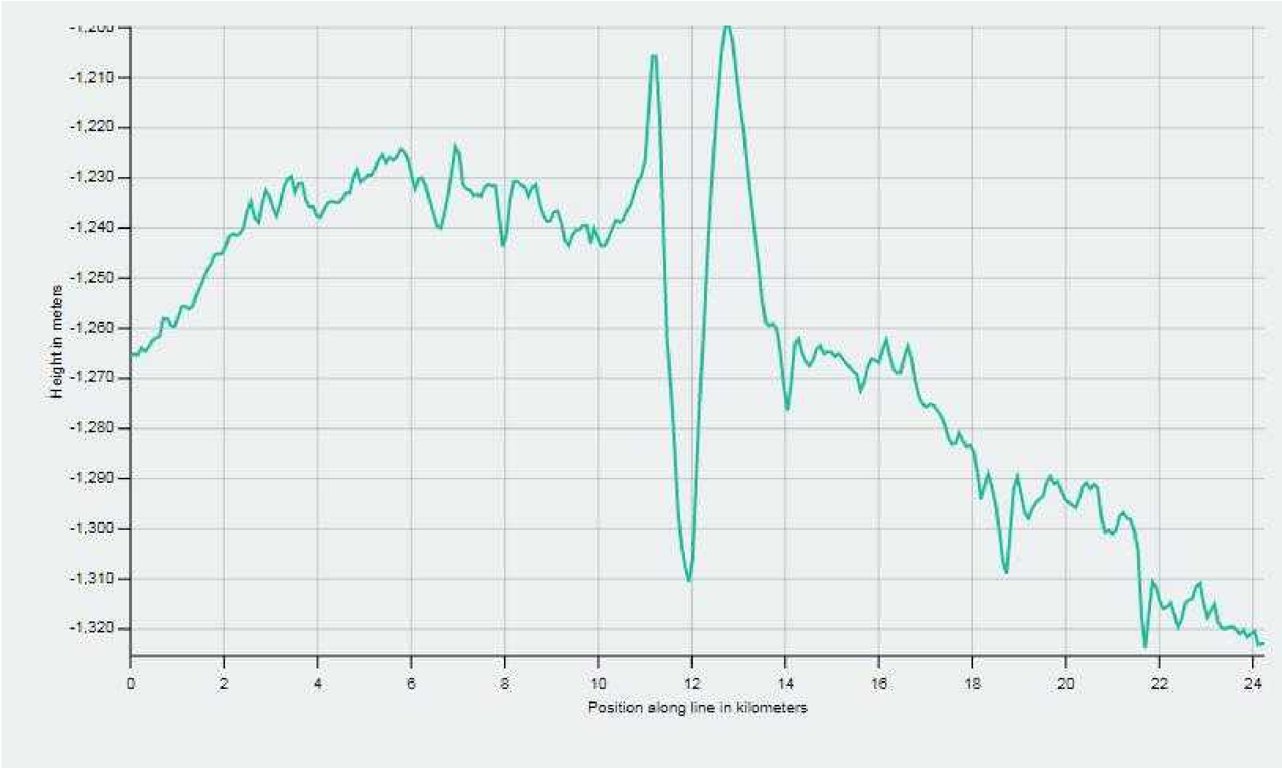

Figure 3: Sectional profile in E-W direction of Prinz 1.

It belongs to class In1 of possible lunar intrusive domes (Fig. 4). The first class, In1, comprises large domes with diameters above 25km and flank slopes of 0.2°–0.6°, class In2 is made up by smaller and slightly steeper domes with elongated shapes and diameters of 10–15 km and flank slopes between 0.4° and 0.9°. Domes of class In3 have diameters of 13–20 km and flank slopes below 0.3°.

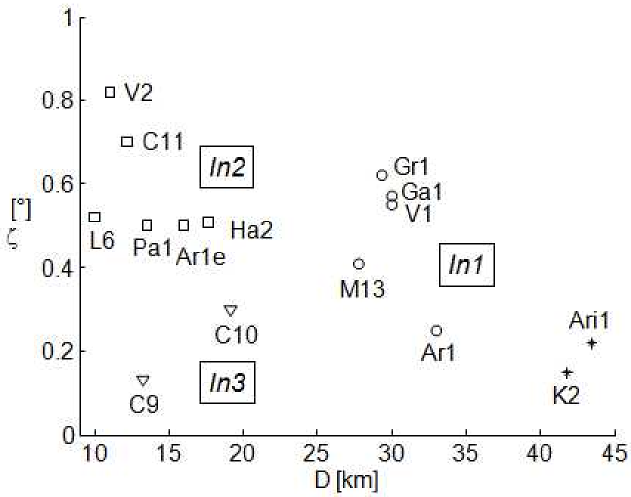

Figure 4: Diameter D vs. flank slope ζ diagram (indicating the dome classes In1–In3) of the candidate intrusive domes as introduced in [5-8].

To estimate the geophysical parameters of lunar intrusive domes, especially the intrusion depth and the magma pressure that occurred during their formation, the laccolith model by Kerr and Pollard [9] has been used.

Intrusive domes of class In1 are characterised by uppermost basaltic layer thicknesses of 0.3-0.6 km and more, intrusion depths of 2.3-3.5km and magma pressures of 18-29MPa. For the smaller and steeper domes of class In2, the uppermost basaltic layer has a thickness of typically only 0.1-0.2 km, the magma intruded to shallow depths between 0.4 and 1.0km while the inferred magma pressures range from 3 to 8MPa. Class In3 domes are similar to those of class In1 with similar thicknesses of the uppermost basaltic layer ranging from 0.4 to 1.2km, intrusion depths of 1.8-2.7 km and magma pressures of 15-23MPa.

For Prinz 1 I have computed, using the geophysical models [5, 8], a thickness of the uppermost basaltic layer of 0.47km, an intrusion depth of 2.3km and a maximum magma pressure of 27 MPa. It is an interesting object for lunar observers to improve their knowledge on the lunar domes.

References

[1] Pollard, D.D., Johnson, A.M. (1973), ‘Mechanics of growth of some laccolithic intrusions in the Henry Mountains, Utah. Bending and failure of overburden layers and sill formation.’ *Tectonophysics* 18:311–354.

[2] Head, J.W., Murchie, S.L., Prockter, L.M., Solomon, S.C., Strom, R.G., Chapman, C.R., Watters, T.E., Blewett, D.T., Gillis-Davis, J.J., Fassett, C.I., Dickson, J.L., Hurwitz, D.M., Ostrach, L.R. (2009). ‘Evidence for intrusive activity on Mercury from the first Messenger flyby.’ *Earth and Planetary Science Letters* 285:251–262.

[3] Ollier, C. (1988), *Volcanoes*. Basil Blackwell, Inc., New York,

[4] Peterson D.W., Tilling, R.I. (2000). ‘Lava Flow Hazards.’ In: Sigurdsson H (ed.), *Encyclopedia of Volcanoes*, Academic Press, San Diego:957–972

[5] Lena, R., Wöhler, C., Phillips, J., Chiocchetta, M.T., 2013. *Lunar domes: Properties and Formation Processes*, Springer Praxis Books.

[6] Lena, R., ‘Lunar domes’, chapter in *Encyclopedia of Lunar Science*, ed. Brian Cudnik, 2015, Springer ISBN: 978-3-319-05546-6.

[7] Lena, R., & Wöhler, C., 2008. ‘Intrusive Lunar Domes: Morphometry and Mode of Emplacement.’ Lunar and Planetary Science Conference XXXIX, abstract #1122.

[8] Wöhler, C., & Lena, R., 2009. ‘Lunar intrusive domes: Morphometric analysis and laccolith modelling.’ *Icarus*, 204 (2), 381-398.

[9] Kerr, A. D., & Pollard, D. D., 1998. ‘Toward more realistic formulations for the analysis of laccoliths.’ *Journal Structural Geology, 20* (12), 1783–1793.

GODIN Barry Fitz-Gerald

Whilst not as conspicuous as some of the brighter rayed craters the 34km diameter Godin stands out because of its odd polygonal, almost triangular outline and high albedo walls which are conspicuous at high sun angles (Fig. 1). The presence of a ray system indicates that the crater is reasonably young in lunar terms and formed in the Copernican period which began some 1.1 billion years ago. It sits on a patch of highland terrain to the north of the southern highlands and south of Mare Vaporum, and at full moon is almost central on the lunar disc.

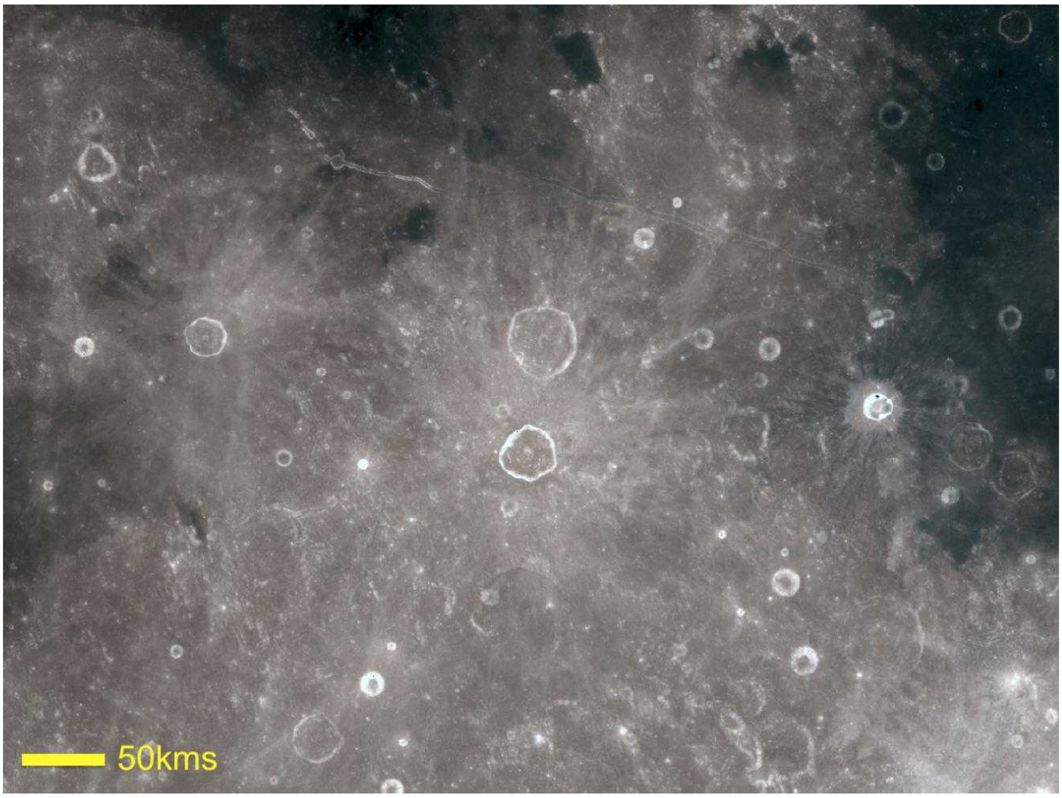

Fig. 1 WAC Hapke-Normalized Colour overlay in LROC Quickmap showing Godin with high albedo inner walls and polygonal outline. Agrippa is just to the north, the bright Dionysius to the east and Horrocks some 200kms away to the south-southwest. Also note another triangular crater, Ukert to the north-west.

The rays are not easy to see against the bright highland terrain, but their structure is more apparent when we look at an image such as Fig. 2 which shows the iron oxide abundance (FeO wt %) overlay from the Kaguya Multiband Imager using the LROC Quickmap website. This shows the asymmetric distribution of ejecta typical of moderately low angles (~35°) which in this case was from the south-west. Such an impact angle would not be sufficient to produce an asymmetric crater and the crater outline must be the result of something else.

Polygonal craters are common amongst complex lunar craters in the 20-45km diameter size range with the shape reflecting the presence of deep crustal tectonic faults and fractures in the target rock. These features are thought to provide lines of weakness preferentially excavated during the cratering process or that influence the collapse of the transient cavity. The exact mechanism involved is still open to debate and not all craters in this size range in a one particular area will end up polygonal. The best known terrestrial example of a polygonal crater is the distinctly square Meteor Crater in Arizona. It's shape is thought to have been influenced by the presence of orthogonal jointing in the target rock, but even here the precise effect of this jointing on the final crater shape is still debated [1]. The most likely explanation for Godin's shape is therefore that either the excavation process *or* the subsequent collapse phase was influenced by pre-existing crustal fractures and faults – but which process had the most effect in the final shape of the crater remains unknown. It is likely that the highlands on which Godin sits was deeply fractured and faulted by the formation of large impact basins such as the Imbrium Basin, and many polygonal craters owe their shape to the presence of these faults and fractures which lurk beneath the highland mega-regolith. Godin is not the only polygonal crater in the area, Agrippa to the north is distinctly polygonal whilst Ukert to the north-west is even more triangular in outline than Godin. Unfortunately there are no obvious surface features such as graben or faults that correspond in orientation to the straighter sections of Godin's rim, though the north-eastern rim may line up with the Imbrium Sculpture which is almost radial to the Imbrium basin.

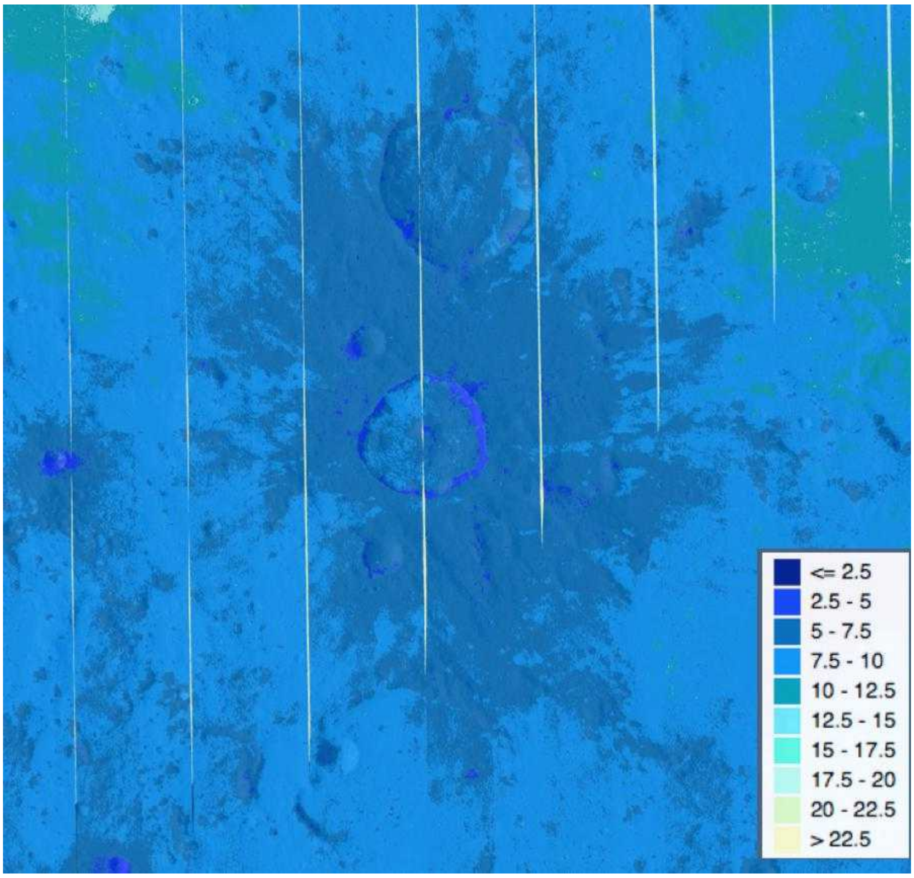

Fig. 2 Godin and environs (FeO wt %) as displayed in the Kaguya Multiband Imager available via the LROC Quickmap website showing the asymmetric distribution of the ejecta. Impact direction was from the south-west (lower left). The darker blue colours corresponds to rocks of highland composition which have a low iron content.

Godin's floor and the lower slopes of its central peak are completely obscured by rocky debris which has collapsed off the crater walls. This debris is marked by a complex of crescentic ridges mostly concave towards the crater centre, each marking a separate wedge of rim that has collapsed down onto the crater floor. Most of these wedges appear to have come off the south-western and north-eastern walls – which is coincidentally the up-range to down-range impact direction (Fig. 3). The ridges are packed tightly one behind the other suggesting that they slid down one after the other in rapid succession during the crater collapse phase. A crater of Godin's size should be a shade over 3kms deep but much of the interior is considerably shallower as a result of the depth of debris covering the floor. A topographic profile shows that the collapse has been more extensive in the south-west where the slumped material reaches up to and over the lower slopes of the central peak (Fig. 4). There is a large slump off the northern wall but this appears to represent one massive collapse as opposed to a series of smaller ones. A smaller collapse off the southern wall also appears to represent a single event.

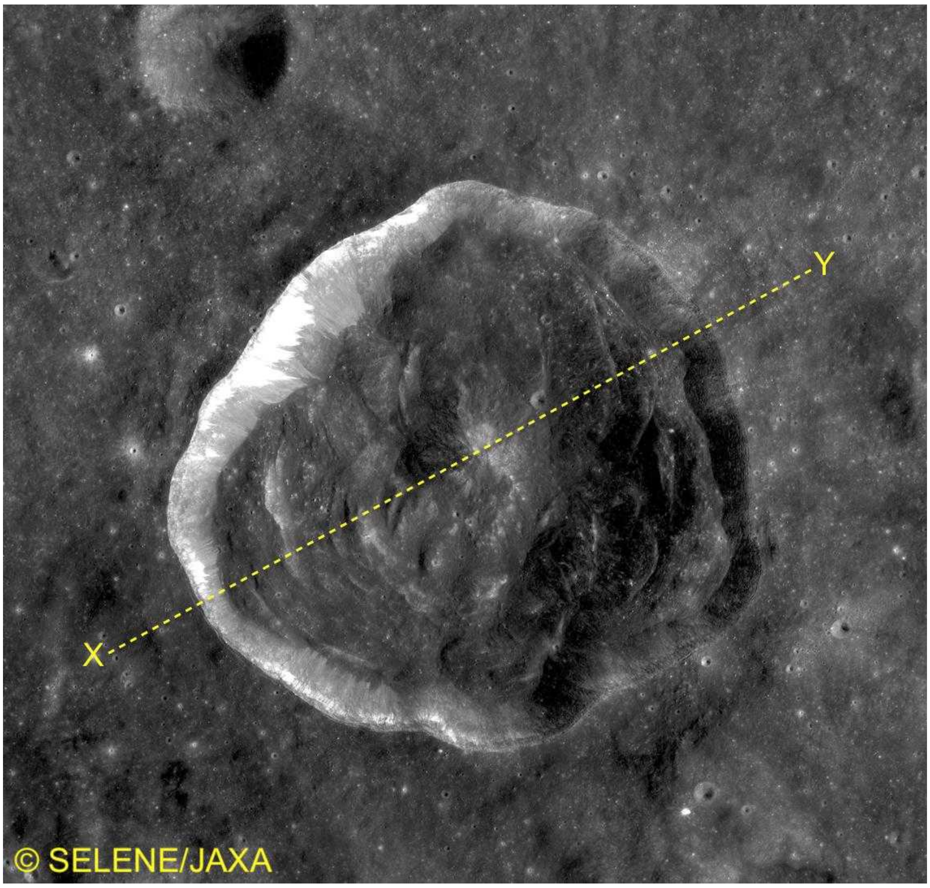

Fig. 3 SLENE/JAXA image of Godin showing the crescentic ridges of successive wall collapses principally from the SW and NE directions. The topographic profile along line X-Y is shown in Fig.4. Note extremely bright avalanches superimposed on older ones below the north-western rim.

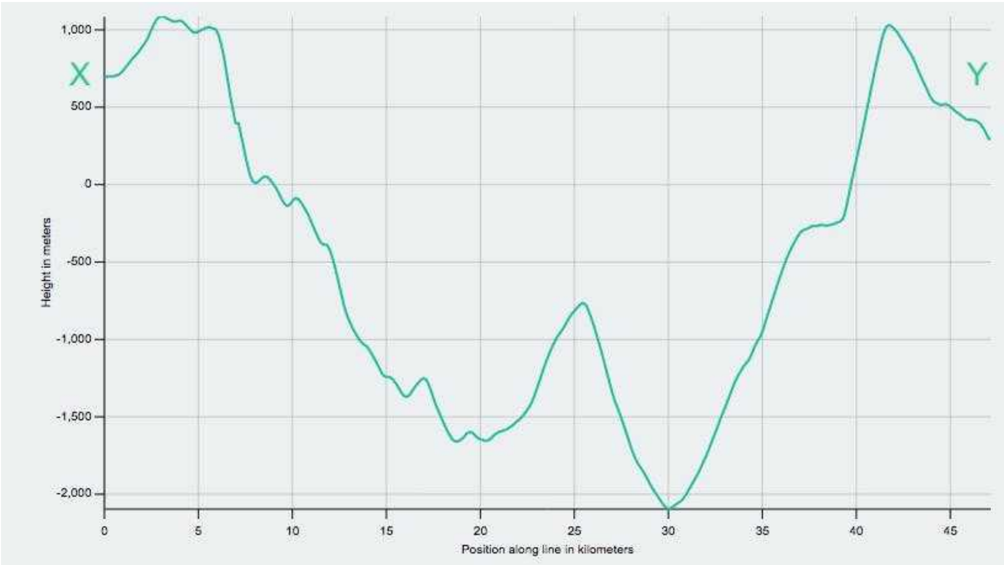

Fig. 4 Topographic profile (SLDEM2015+LOLA(m)) along line X-Y in Fig.3 produced from LRO Quickmap. Note more extensive collapse from the SW.

Most young complex lunar craters show at least a hint of an impact melt covered crater floor but Godin is unusual in that no trace of such a floor is visible. This indicates that the extent of the crater wall collapse was much greater here than in other craters. As with the polygonal outline this may be a result of the properties of the target rocks at 'ground zero'. Agrippa to the north looks like it has some of its original crater floor preserved to the east of the central peak, but this is just a flat area of collapse debris some 500m above that the actual floor. This shows that Agrippa has also experienced a substantial crater collapse phase, possibly due to the same factors seen in Godin.

The Optical Maturity image in Fig. 5, shows where avalanches of boulders and finer material (colour coded red and yellow) have cascaded down the crater walls, and it is this fresh rocky material that makes Godin's walls so conspicuous at full moon. These deposits remain optically immature because they are constantly rejuvenated with 'unweathered' material which is exposed as the boulders, rock and finer material move slowly and occasionally rapidly downslope. Some of these avalanches end in a 'cat's paw' morphology [2] which suggest a simultaneous collapse along quite a broad front. Fig. 6 shows an example which may have been triggered by the impact of a cluster of secondary craters on the adjacent section of rim. The source of the rocks in these these avalanches include layers of exposed local bedrock just below the crater rim and material that makes up the rim itself.

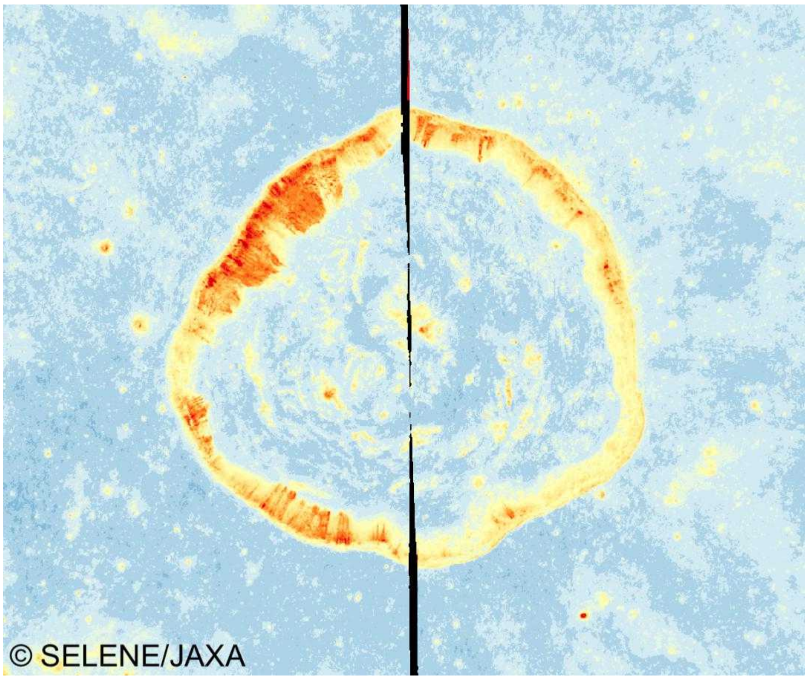

Fig. 5 Derived Optical Maturity (OMAT) mosaic of Godin created from topographically-corrected Mineral Mapper reflectance data acquired by SELENE/Kaguya. Red's are optically immature deposits and individual avalanches down the walls can easily be seen, particularly to the north-west.

This avalanche activity has been going on for a long time as many of the younger avalanche trails lie on top of or cut across older ones. Numerous fractures are visible on the crater glacis (the slopes immediately outside the rim) running parallel to and immediately outside the crater rim. Fractures like these are responsible for all the debris that ends up collapsing down onto the crater floor, and are probably a constant source of falling rocks and boulders. What can also be seen is that the glacis is draped in impact melt which has broken up in to lots of sub-rectangular blocks, which is typical of a melt veneer when placed under tension. Debris eroding from different heights up the crater wall account for the observation that some of the avalanches are dominated by material of a low iron content and probably derived from plagioclase rich anorthosite exposed just below the crater rim, and some are dominated by material of a higher iron content which is probably derived from the melt veneer and ejecta on the crater rim.

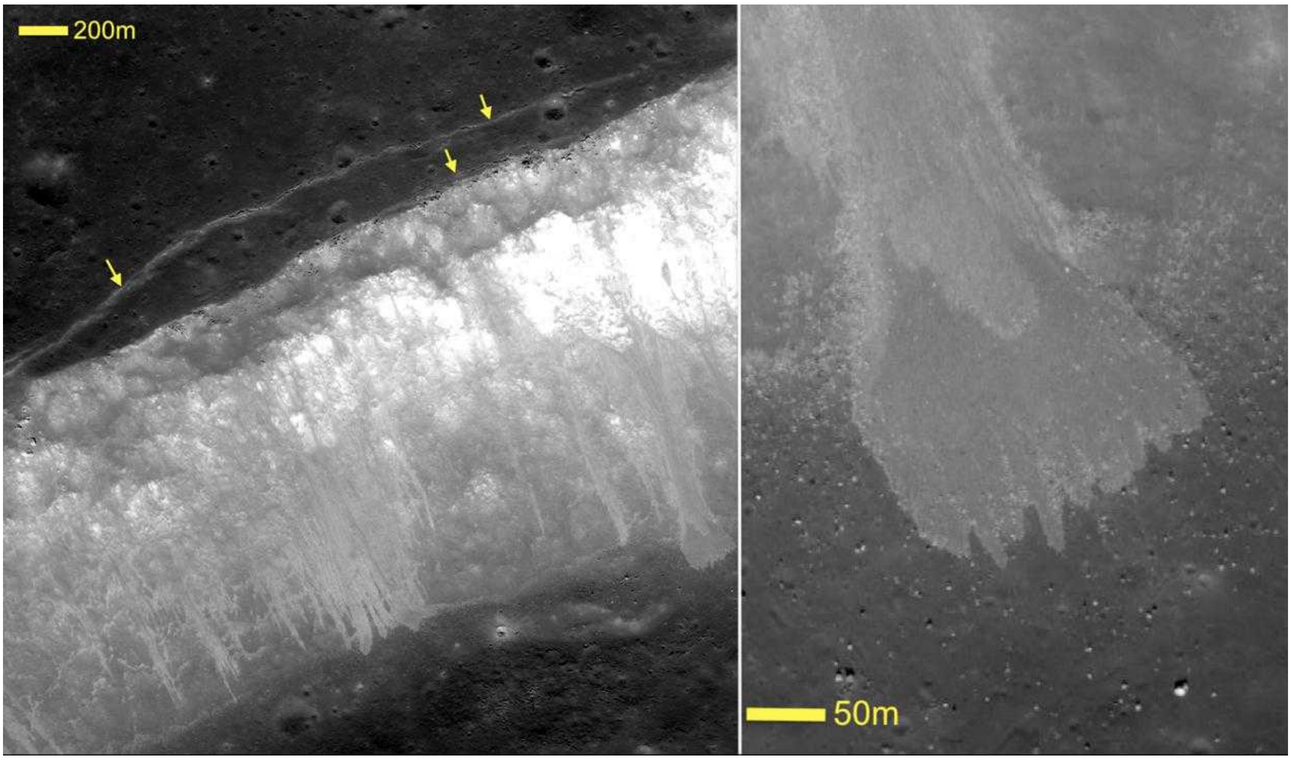

Fig. 6. Left - LROC NAC image of a section of the south-western rim of Godin showing complex avalanches down the inner wall derived from bedrock exposed in the crater rim and material off the rim. Fractures running parallel to the rim (yellow arrows) can be seen on the glacis, with the edges of the fractures having the blocky appearance typical of impact melt. Right – detail of an avalanche ending in a 'cat's paw' (named so for obvious reasons!) indicative of simultaneous collapse on a broad front.

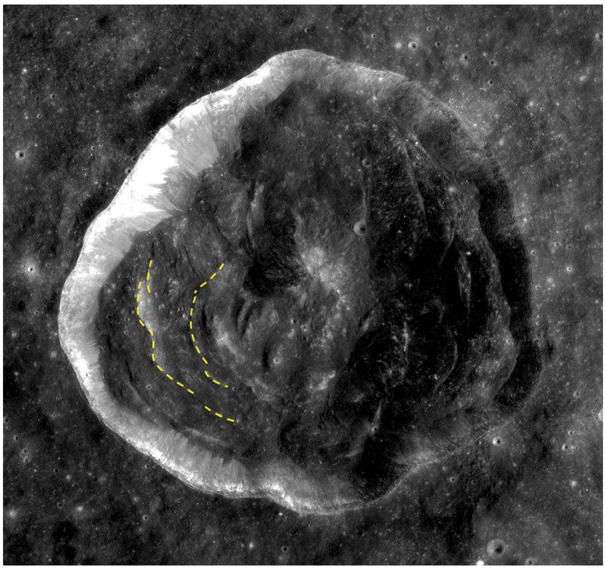

Fig. 7 Crescentic ridges to the west of the central peak of Godin (yellow dashed lines) that could have been responsible for the report of a ruined ring on the crater floor.

As mentioned above, the slumps on the crater floor are marked by crescentic ridges each of which represent a slumped block of crater wall. The ridges closest to the central peak represent the first slumps, with later ones pushing the first ones further in towards the middle of the crater floor. The presence of these curved ridges may explain an observation made by Patrick Moore using the Meudon 33-inch refractor on 21st April 1953 [3]. He observed '*the remains of a ruined ring on the floor, east of the central elevation*'. As of 1961 the International Astronomical Union standardised the lunar cartographic nomenclature to have north in the 'up' direction so in this description we need to substitute 'east' for 'west' and look to the west of the peak for any trace of this suspected ring..

None of these ridges describe a complete circle, and there is clearly no such ring-like structure to the west of the central peak in the recent imagery. The crescentic ridges could however easily lead to the impression that they defined one side of a complete ring shaped structure (Fig. 7). It is possible that the observer inferred the presence of a complete circle by linking up several separate curved sections in to a single circular structure, a phenomenon that the human eye and brain are particularly adept at doing when insufficient visual information is available.

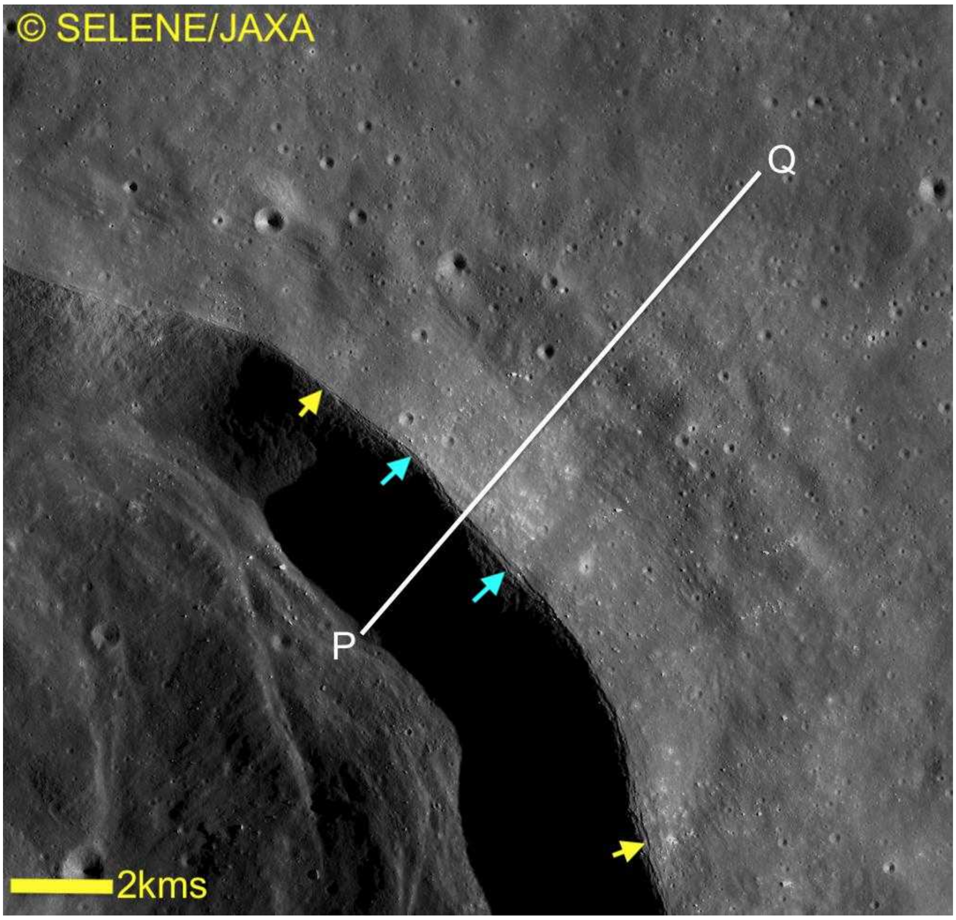

Fig. 8 SELENE image of the north-eastern rim of Godin showing the outwards slump (between yellow arrows) and patch high albedo of anorthosite bedrock (between blue arrows) exposed on the crater rim. An elongate debris mount can be seen below the slump scar.Topographic profile P-Q is shown in Fig.9. Note 'ripples' of impact melt on the side of the debris mound facing the crater.

Slumping is not restricted to inside the crater and an approximate 10km section of the north-eastern rim has slumped outwards down the glacis (Fig. 8) producing a slump scar on the rim and an elongate debris mound further down the glacis (Fig. 9). This probably occurred during the crater collapse phase as ripples of solidified melt can be seen on the surface of the mound facing the crater rim, and for this to be visible the mound would have to have been in place before the melt was pushed outwards over the rim as the inner walls slumped down in to the impact melt lake. Part of this slump has exposed anorthosite bedrock in the form of a 2km long high albedo patch on the north-eastern glacis. Some high resolution amateur images show a hint of this patch under morning illumination in the form of a brighter section on the glacis, though I imagine it would be a subtle target visually. The debris mound can also be seen in some of these images, but again this would probably be a difficult target as it is only some 150m high.

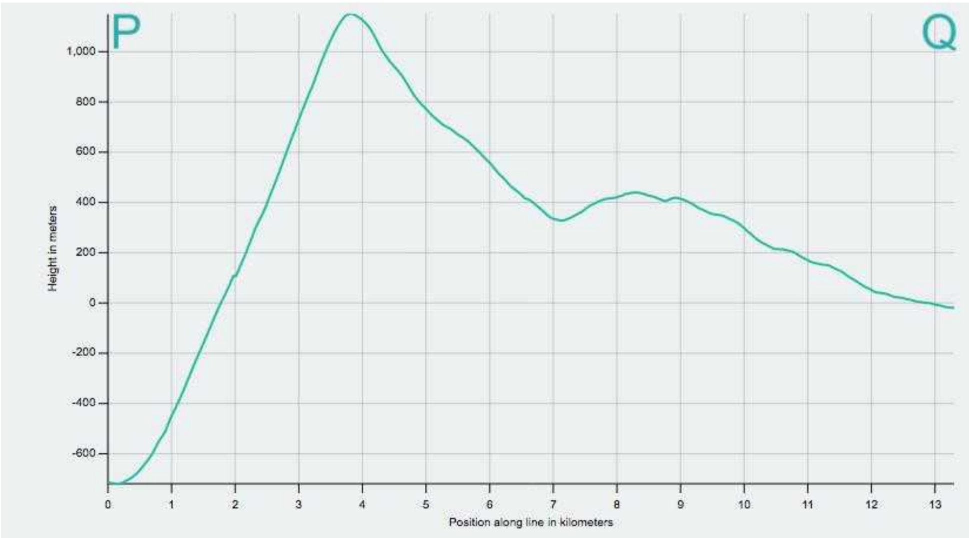

Fig. 9 LROC Quickmap topographic profile along line P-Q in Fig.8. Note the conspicuous debris mound on the glacis.

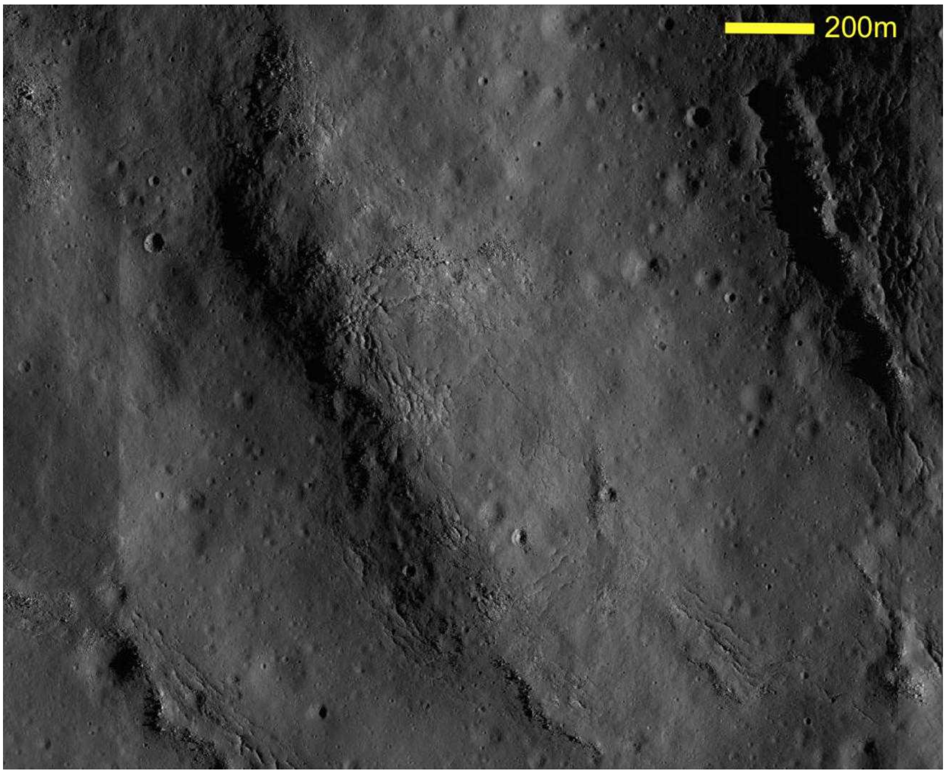

Fig. 10 One of the crescentic ridges on the western floor of Godin showing the presence of a widespread impact melt veneer. Note the 'crazy paving' pattern as the veneer fractures along cooling cracks and along the ridge crests.

A closer look at the interior of Godin reveals that all the slumped debris on the floor is coated with a veneer of impact melt. This is now fractured into rectangular blocks along the crests of the ridges and on steeper slopes, and where erosion has opened up the abundant shrinkage cracks that formed on the cooling melt surface (Fig. 10).

The presence of this melt veneer indicates that the wall slumping occurred whilst the impact melt was molten and still relatively mobile. As each successive wedges of wall material collapsed it would have slid downward in to the impact melt lake on the crater floor to form a rock/melt mush as it sank in to the lake. A substantial amount of melt also ended up forming a thin veneer over the surface of all this collapsed material. Some melt was thrown up and over the rim and on to the glacis to form a veneer there as well. Melt can also be seen on the central peak, and it is possible that it was at one time completely draped in this material. This is indicated by the presence of what appears to be a melt 'flow' some 3kms long snaking down the 11° slope of the northern flank (Fig. 11) to spread out in a broad fan at its base. This probably formed as melt drained off the summit and coalesced into one broad flow, cooling as it did, but retaining sufficient mobility for it to flow down the gentle slope towards the crater floor. There were probably other similar flows draining melt off other parts of the summit, but this is the most prominent. A comparable situation exists in the crater Romer [4], where the central peak and a zone around it are covered in solidified melt, but the distribution here is nowhere near as extensive as that seen in Godin.

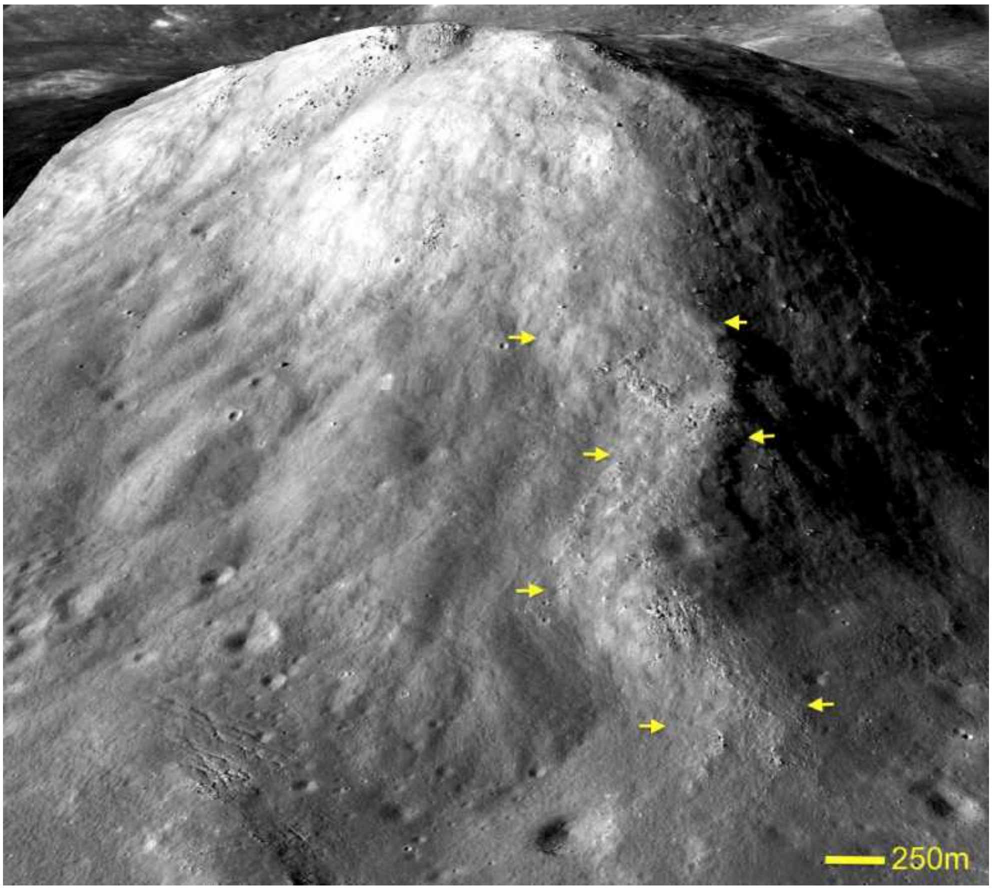

Fig. 11 Impact melt flow (yellow arrows) which flowed down the northern flank of the central peak. 3D rendition from LROC Quickmap.

In summary Godin was formed by a low angle impact from the south-west which struck fractured highland terrain on the edge of the Imbrium Basin some time in the Copernican period. The crater-forming process was affected by the inhomogeneous nature of the target area which was deeply faulted and fractured, and these lines of weakness influenced the excavation of the crater or its subsequent modification during the collapse phase. An impact melt lake formed on the crater floor, but this was rapidly filled in as the crater walls collapsed. This occurred in a rapid series of events as thin wedges of rim separated along curving fracture lines and slid down on to the crater floor. This debris slid down and sank in the molten lake and also displaced some of the melt, pushing it up and over the central peak and in places over the crater rim itself. Part of the crater's north-eastern rim collapsed outwards during this phase exposing the anorthosite bedrock on the crater glacis. The crater walls continued to collapse inwards bit by bit until the crater floor and the lower slopes of the central peak were completely buried in debris and the original melt lake completely filled in. Melt formed a thin veneer over the slumped debris and this eventually solidified to form a solid carapace. As it cooled and contracted it fractured and cracked and eventually broke up along lines of stress in to a myriad of small rectangular boulders. The final phase of Godin's history consisted of a succession of boulder avalanches and flows of finer granular material which cascaded down the crater walls from bedrock exposed in the crater rim and off the rim itself. This process is still active and keeps the walls bright as fresh rock surfaces are continually exposed by gradual movement towards the crater floor.

Barry Fitz-Gerald. (barryfitzgerald@hotmail.com)

Acknowledgements:

LROC images reproduced by courtesy of the LROC Website at http://lroc.sese.asu.edu/index.html, School of Earth and Space Exploration, University of Arizona.

Selene images courtesy of Japan Aerospace Exploration Agency (JAXA) at:
http://l2db.selene.darts.isas.jaxa.jp

References:

1.Öhman,T.,et.al.(2010) 'Polygonal impact craters in the Solar System: Observations and implications.' Chapter in *Special Paper of the Geological Society of America* 465:51-65

2 Kokelaar, P.,et.al. (2017). 'Granular avalanches on the Moon: Mass-wasting conditions, processes and features.' *Journal of Geophysical Research: Planets*. 122. 10.1002/2017je005320.

3. Wilkins, H.P and Moore, P. (1961), *The Moon: A Complete Description of the Surface of the Moon*. Faber&Faber, 1958, p. 55.

4. 'Central peak of Römer', BAA Lunar Section Circular, Vol. 49, No. 12, December 2012.

LUNAR OCCULTATIONS February 2020

Tim Haymes

Overview

The Moon starts the month in Cetus, a day before 1st Quarter. On Feb 2nd 08h UT, (4)Vesta is 5' arc North of the lunar limb (daylight). An occultation can't be seen *from the UK* unfortunately, but observers in Japan, Eastern Russia and Alaska should. There are no UK observable occultations of the big 4 asteroids out to 2030, so please don't hold your breath for any of these. The Moon passes north of the Hyades on Feb 3/4 and occults 106 Tau on the evening of the 4th. A Southern Limit Graze is predicted across Devon and Cornwall (BAAH #2 ZC765). Predictions can be found here https://britastro.org/downloads/17673

The number of predictions increases as the Moon traverses Gemini, and on Feb 6th eta and mu are again hidden. On the morning of the 8th the 97% illuminated phase occults mu Cancri. There are predictions for 7th and 8th magnitude stars around Full Moon which are observable visually in good optics. XC 1250 (HIP 40866) on the Feb 8th 0350 UT is at magnitude 5.2 R and close to grazing incidence near Oxford. There are no graze predictions for this due to the lunar phase, but would be worth monitoring from S England. It is occulted from Manchester areas.

In the following days the Moon passes through Virgo and into Libra.

Fl-24 Virginis makes an emergence on Feb 14 at 0519UT. There are fewer predictions now while we wait for the next lunation.

On Feb 25th 1839UT there is a graze of 33 Pisces across Scotland and Northern Ireland (BAAH #4 ZC 5). The star isn't occulted south of the limit. The Moon is crescent phase and should be dramatic to those in the graze zone. See the britastro link above for the prediction.

SPECIAL EVENT DD of ZC1014 March 4th

This is a new suspect double star, and observation of it would be very useful. It was reported as possibly double in a video recording made by Bod Sandy (IOTA-US) on April 20, 2010. This is the last opportunity until events resume in 2028 AD. Video or visual welcomed.

QHY174m-GPS

I now have this USB3 CMOS camera which has internal GPS time stamping of frames. I plan to test it on lunar occultations this month. However, I will continue to use *video/GPS-VTI* for routine lunar occultations because this is the timing 'gold standard'. My intention is to use the QHY for fast recordings of some lunar events (e.g. double stars) at 200 fps. I shall also be checking if there is a time differential between USB3-CMOS and Video. This will involve two telescopes, an 8" F/4 and a C11. More next month – clear skies – Tim (Coordinator)

2020 February predictions for Manchester (Occult4 by D.Herald).

W. Longitude 002d 15', Latitude +53 25', Alt. 50m, aperture 25 cm.
Events excluded: Daytime, Bright-limb

y	m	day d	Time h	m	s	P		Star No	Sp	Mag v	Mag r	% ill	Elon	Sun Alt	Moon Alt	Moon Az	CA o	Notes
20	Feb	1	21	11	38.3	D		110632	K5	9.0	8.4	48+	87		32	240	86N	
20	Feb	1	23	33	50.2	D		393	K0	6.7	6.1	49+	88		13	271	35N	Dbl*
20	Feb	2	0	43	9.9	D		398	K0	6.5*	5.9	49+	89		3	284	66S	Dbl*
20	Feb	2	17	49	25.5	D		475	A0	7.5*	7.5	56+	97	-9	50	161	51N	
20	Feb	3	17	35	14.9	D		610	K5	6.1	5.1	66+	109	-6	48	139	87N	
20	Feb	3	18	6	43.3	D		93781	A0	7.6*	7.6	66+	109	-11	51	149	64S	
20	Feb	3	20	38	22.4	D		93811	K2	8.5	7.8	67+	110		52	208	71N	
20	Feb	3	23	56	44.6	D		629	G5	7.5*	7.2	68+	111		29	262	47N	
20	Feb	4	1	41	25.8	D		643	F6	6.8	6.6	69+	112		14	282	42N	
20	Feb	4	21	30	0.4	D		765	A5	5.3	5.2	77+	122		55	209	37S	106 Tau
20	Feb	4	22	7	9.5	D		76982	F0	8.4	8.2	77+	123		51	222	51S	
20	Feb	4	22	23	1.0	D		76985	A2	8.0	7.9	77+	123		50	227	28S	
20	Feb	4	23	6	11.2	D		77012	F0	7.8	7.6	77+	123		45	240	49S	
20	Feb	5	19	26	18.5	D		911	B8	6.4	6.4	85+	134		53	137	50N	141 Tau
20	Feb	5	20	5	9.9	D		77887	F8	8.2	7.9	85+	134		57	151	71N	
20	Feb	5	20	7	25.2	D		77891	K2	8.2	7.4	85+	134		57	152	76N	
20	Feb	5	20	7	53.4	D		77877	B9	8.0	8.0	85+	134		57	153	30S	
20	Feb	5	22	29	58.4	D		77976	K2	8.5	7.8	85+	135		56	212	37S	
20	Feb	5	22	49	31.8	D		77991	K5	8.7	7.8	86+	135		55	219	36N	
20	Feb	5	23	47	57.9	D		928	K4	5.9	5.1	86+	136		48	237	37S	
20	Feb	6	2	11	9.9	D		946	M3	3.5	2.5	86+	137		28	270	62N	eta Gem
20	Feb	6	2	11	10.3	D	X	85102		6.1	5.5	86+	137		28	270	62N	
20	Feb	6	3	22	34.3	D		78182	G5	7.4	6.9	87+	137		18	283	36S	
20	Feb	6	5	29	12.2	D		976	M3	2.9	2.0	87+	139		2	307	39N	mu Gem

20	Feb	6	17	43	54.0	D		1059	G5	6.9*	6.6	92+	146	-7	33	96	50S	Dbl*
20	Feb	6	21	5	8.3	D		1078	B8	6.0	6.0	92+	148		57	152	69S	44 Gem
20	Feb	6	21	33	3.0	D		79056	G0	8.3	7.9	92+	148		59	163	80S	
20	Feb	6	22	6	12.0	D		79070	S3	7.5	6.4	92+	148		59	178	85S	
20	Feb	6	22	24	33.4	D		79067	M0	8.4	7.6	92+	148		59	186	33S	
20	Feb	7	18	48	17.9	D		79884	K0	8.0	7.2	97+	160		33	97	52N	
20	Feb	7	19	25	7.1	D		79909	K0	7.6	7.0	97+	160		38	105	78N	
20	Feb	7	21	14	51.2	D		1224	G2	5.3*	5.0	97+	161		52	135	84S	mu Cnc
20	Feb	8	1	19	16.5	D		80039	A5	8.4	8.3	98+	163		50	229	32S	
20	Feb	8	1	48	8.5	D		80063	G5	7.6	7.1	98+	163		47	237	85N	
20	Feb	8	3	6	1.0	D		80094	K2	8.0	7.4	98+	163		36	256	42N	
20	Feb	8	3	17	57.8	D		80099	B9	8.1	8.2	98+	164		34	259	68S	
20	Feb	8	3	51	10.7	D		1250	K1	5.8	5.2	98+	164		30	265	31S	Graze?
20	Feb	9	20	58	34.3	R		1485	G0	7.1	6.8	99-	171		30	105	87S	
20	Feb	10	21	27	30.5	R		1612	F5	7.3	7.1	96-	157		22	103	83N	
20	Feb	10	23	56	2.0	R		1622	K2	8.2*	7.6	96-	156		40	138	37N	
20	Feb	12	2	16	48.8	R		119272	F5	7.6*	7.3	89-	141		39	167	79S	
20	Feb	13	3	1	17.8	R		139174	F2	7.8*	7.6	80-	126		33	166	73S	
20	Feb	13	5	54	50.9	R		139229	K2	7.3	6.6	79-	125		28	215	48S	
20	Feb	14	1	16	54	Gr		2008	K0	6.6*	6.0	70-	114		15	128	10S	Dbl*
20	Feb	14	2	2	18.7	R		139675	K0	8.1*	7.6	70-	113		20	139	79S	
20	Feb	14	5	19	47.5	R		2020	A0	6.5	6.5	69-	112		27	191	66S	94 Vir
20	Feb	14	6	24	24.4	R		139753	MB	8.3	7.5	68-	111	-10	24	207	47N	
20	Feb	16	5	33	51.7	R		2277	K0	8.2	7.6	46-	86		18	168	66N	
20	Feb	18	5	53	26.7	R		185780	F0	7.9	7.7	26-	61		8	149	47N	
20	Feb	25	18	43	16	M		5	K1	4.6	4.1	4+	23	-10	6	252	16S	33 Psc
20	Feb	26	20	3	40.4	D		128992	K0	8.7	8.1	9+	34		5	263	82S	
20	Feb	27	18	17	19.5	D		109952	K0	7.4*	6.6	14+	44	-6	28	234	37S	
20	Feb	27	19	24	36.4	D		109982	F5	8.2*	7.9	15+	45		20	250	86N	
20	Feb	27	20	43	24.9	D		236	K0	8.0	7.3	15+	45		9	266	81S	
20	Feb	28	21	9	40.8	D		345	F0	7.6		22+	56		14	266	74S	
20	Feb	29	20	44	15.5	D		454	K3	5.6*	5.1	31+	67		28	254	67N	
20	Feb	29	21	40	2.8	D		93292	K0	8.1*	7.5	31+	68		20	266	77S	
20	Feb	29	23	12	17.0	D		93323	A2	8.6*	8.4	32+	68		7	284	69N	
20	Mar	1	20	16	37.2	D		93654	K0	8.3	7.7	40+	78		41	240	49N	
20	Mar	1	20	34	49.5	D		581	G0	6.8*	6.4	40+	78		38	244	43S	
20	Mar	1	21	2	8.2	D		93671	K2	9.0	8.5	40+	79		35	251	55N	
20	Mar	1	22	52	52.5	D		93701	F8	8.3*	8.0	41+	79		19	274	74N	
20	Mar	1	23	55	4.4	D		590	A0	6.3	6.3	41+	80		10	285	51N	
20	Mar	2	22	55	31.0	D		94154	K0	8.5	7.9	51+	91		28	267	69S	
20	Mar	3	18	56	36.9	D		77324	B8	8.9	8.8	60+	101	-10	59	179	25N	
20	Mar	3	19	9	30.9	D		77342	M0	8.6	7.8	60+	101		59	184	89S	
20	Mar	3	19	17	15.5	D		77344	A5	9.0	8.8	60+	101		59	188	66N	
20	Mar	3	20	6	22.1	D		851	A1	6.4*	6.4	60+	102		56	208	43S	Dbl*
20	Mar	3	22	19	58.6	D		77460	K7	8.4	7.4	61+	102		42	249	53S	
20	Mar	3	22	24	27.6	D		77469	B8	8.6	8.5	61+	102		41	250	72S	
20	Mar	4	0	7	20.0	D		77553	G0	8.1*	7.8	61+	103		26	272	47S	
20	Mar	4	19	49	27.4	D		1014	A0	7.0	7.1	70+	114		60	178	49N	SPECIAL
20	Mar	4	20	31	21.3	D		78561	K2	7.4	6.6	70+	114		59	196	35S	
20	Mar	4	22	1	9.3	D		78627	K2	8.9	8.2	71+	115		52	229	79S	
20	Mar	4	22	26	38.9	D		78628	B9	8.8	8.8	71+	115		49	238	13N	
20	Mar	4	23	35	1.2	D	X	9691	K8	8.6	7.8	71+	115		40	254	62S	
20	Mar	5	0	0	44.5	D		1033	A2	6.8	6.7	72+	115		36	260	88S	
20	Mar	5	0	5	15.9	D		78702	K0	7.8	7.1	72+	116		35	261	79S	
20	Mar	5	20	26	39.0	D		1152	G5	7.0	6.4	80+	127		59	169	49S	Dbl*
20	Mar	5	20	56	32.9	D		79573	M0	8.9	8.0	80+	127		59	182	46S	
20	Mar	5	23	0	45.6	D		79628	F5	7.1	6.9	81+	128		51	230	63S	
20	Mar	5	23	13	19.7	D		1167	K0	6.3*	5.8	81+	128		50	233	74N	
20	Mar	5	23	59	15.0	D		79660	K0	7.6	6.8	81+	128		44	246	45N	

Predictions to magnitude 9.0 completed up to March 5th.

Notes on the Double Star selection.

Doubles are selected from Occult 4, where the magnitudes of the pair are not more than 2 magnitudes different, the fainter companion is brighter than mag 9, and the time difference (dT) is between 0.1 and 5 seconds. **Please report double star phenomena.**

Key:
P = Phase (R or D), R = reappearance D = disappearance
M = Miss at this station, Gr = graze nearby (possible miss)

CA = Cusp angle measured from the North or South Cusp. Negative CA = bright limb
Dbl* = A double star worth monitoring.
Mag(v)* = asterisk indicates a light curve is available in Occult-4
Star No:
1/2/3/4 digits = Zodiacal catalogue (ZC) referred to as the Robertson catalogue (R)
5/6 digits = Smithsonian Astrophysical Observatory catalogue (SAO)
X denotes a star in the eXtended ZC/XC catalogue.
The ZC/XC/SAO nomenclature is used for Lunar work. The positions and proper motions of the stars in these catalogues are updated by Gaia.

Detailed predictions at your location for 1 year are available upon request.
Occultation Subsection Coordinator: Tim Haymes
tvh.observatory@btinternet.com

LUNAR GEOLOGICAL CHANGE DETECTION PROGRAMME 2020 Feb

Tony Cook

Reports have been received from the following observers for Dec: Jay Albert (Lake Worth, FL, USA - ALPO) observed: Aristarchus and Plato. Alberto Anunziato (Argentina, SLA) imaged: Aristarchus, Copernicus, Langrenus, Plato, Proclus, Theophilus, and Tycho. Aylen Borgatello (Argentina - AEA) imaged: Conon, Mons Piton and Proclus. Maurice Collins (New Zealand - ALPO/BAA/RASNZ) imaged: Alphonsus, Aristarchus, Aristillus, Clavius, Copernicus, Eratosthenes, Grimaldi, Heraclitus, Langrenus, Mare Crisium, Mare Nectaris, Oceanus Procellarum, Plato, Rupes Recta, Theophilus, Triesnecker and captured some whole Moon images. Philip Denyer (London, UK – BAA) imaged Herodotus. Walter Elias (Argentina - AEA) imaged: Mare Crisium, Proclus, Wilkins and several features. Victoria Gomez (Argentina - AEA) imaged: Aristarchus. Facundo Gramer (Argentina - AEA) imaged: Alphonsus, Aristarchus, Secchi, and Timocharis. Gabriel Re (Argentina – AEA) imaged: Aristarchus and Proclus. Trevor Smith (Codnor, UK – BAA) observed visually: Alphonsus, Archimedes, Aristarchus, Censorinus, Fra Mauro, Gassendi, Hyginus, Mare Vaporum, Oenopides, Pallas, Plato, Proclus, Promontorium Laplace, Sirsalis, Timocharis, Torricelli, and Vallis Schröteri. Bob Stuart (Rhayader, UK – BAA) imaged: Aristarchus, Babbage, Cavendish, Copernicus, Damoiseau, Hevelius, Lacus Excellentiae, Mare Insularum, Mersenius, Pythagoras, Schickard, Schiller, Sirsalis, and several features. Aldo Tonon (Italy – UAI) imaged Censorinus.

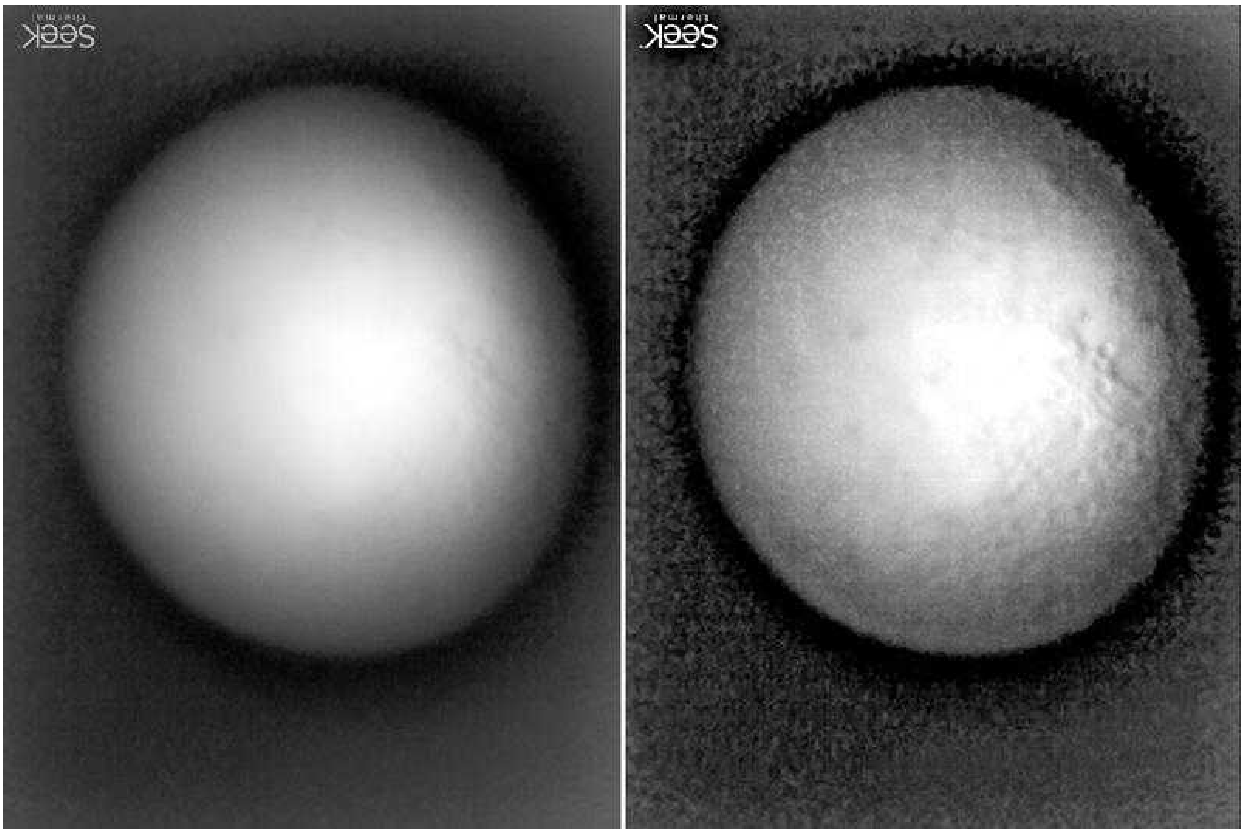

Figure 1. *The disk of the gibbous Moon captured on 2020 Jan 13 UT 04:41 in the Thermal Infrared (7.2-13µm) by Tony Cook, using a 20cm f/8 reflector with thermal IR eyepiece projection. White is hot, dark is cold.* ***(Left)*** *A raw image.* ***(Right)*** *A high pass filtered image.*

News: I received a very useful present at Christmas, a Seek Thermal Compact Pro High Resolution camera for Android phones. Technically speaking I would not call 320x240 high resolution, but it seems cost effective compared with larger format 640x480 cameras by other manufacturers, which are very pricy, and is somewhat better resolution than FLIR ONE Pro cameras at 160x120 pixels. Unfortunately, the camera came with a lens attached which I was reluctant to remove in case I broke the camera. Therefore, I decided to do what many people do with Smart phones, literally put the camera up to the eyepiece in a holder. Alas glass eyepieces do not transmit thermal IR, nor do SCT telescopes with glass corrector plates, so Newtonians with special eyepieces are needed. The camera was fitted onto my 8" f/8 Newtonian and to get around the glass eyepiece problem, a laser cutter lens, made of ZnSe, was ordered up as a 1" thermal IR eyepiece.. This was placed into the eyepiece draw tube and projected an image into the thermal imaging camera. First results were not encouraging (Fig. 1 – Left). You can see the heat from the drawtube, the image is a bit saturated, and pixel sizes are something like 12 x 12 km on the lunar surface. The Moon looks a bit like a featureless orange. Darryl Williams in his past two ALPO TLO articles (See the Sep and Nov 2019 TLO newsletter) has recommended flat fielding to remove these artefacts. I was not quite ready to do this on my first proper observing run with the camera, so instead have tried out some high pass filtering to bring out more detail. You can just about make out Theophilus, Mare Crisium and the edges of some other mare areas in the high pass filtered version of the image in Fig. 1 (Right). Anyway, I will work on ways to get the resolution up and join in with this new observing technique that Darryl has been investigating.

TLP reports: No TLP reports were received in December.

Routine Reports: Below are a selection of reports received for Dec that can help us to re-assess unusual past lunar observations – if not eliminate some, then at least establish the normal appearance of the surface features in question. Note that some observations sent in have not been used in this newsletter because they do not cover repeat illumination predictions. However, they will be kept in our database and used as reference images should a TLP be reported under similar illumination in the future.

Censorinus: On 2019 Dec 02 UT 23:31 Aldo Tonon (UAI) imaged this crater for an ALPO request to find how early in selenographic colongitude the blue colour in this impact colour can be captured on a colour camera.

Aldo seems to have good atmospheric transparency from 19:35-19:44, but after that image contrast worsened as the Moon got lower in the sky. Anyway, a slight turquoise-blue/green can be seen in the ejecta blanket around Censorinus – though there is quite a bit of atmospheric spectral dispersion too in Fig. 2. The colour though vanishes in images after 19:44UT. These are important findings as they suggest the bluishness starts to become visible at least as early as a colongitude of 340.6°, and also the visibility of the colour can be severely affected by observing conditions. This is something we need to take into account when interpreting old TLP reports involving colour.

Figure 2. *A time sequence of images of the crater Censorinus taken by Aldo Tonon (UAI) on 2019 Dec 02 UT 19:35-20:00. All images have had their colour saturation increased to 70%. Images orientated with north towards the top.*

Alphonsus: On 2019 Dec 05 UT 02:22 Facundo Gramer (AEA) imaged this crater under very similar illumination (±0.5°) to the following Russian report:

Alphonsus 1931 Apr 25 UT 18:00 Observed by Vasilev (Russia) "The triang. dark spot close to the w.bank was not vis. after SR & appeared along the length of the term., 8-9 deg" NASA catalog weight=1. NASA catalog ID #401. ALPO/BAA weight=1

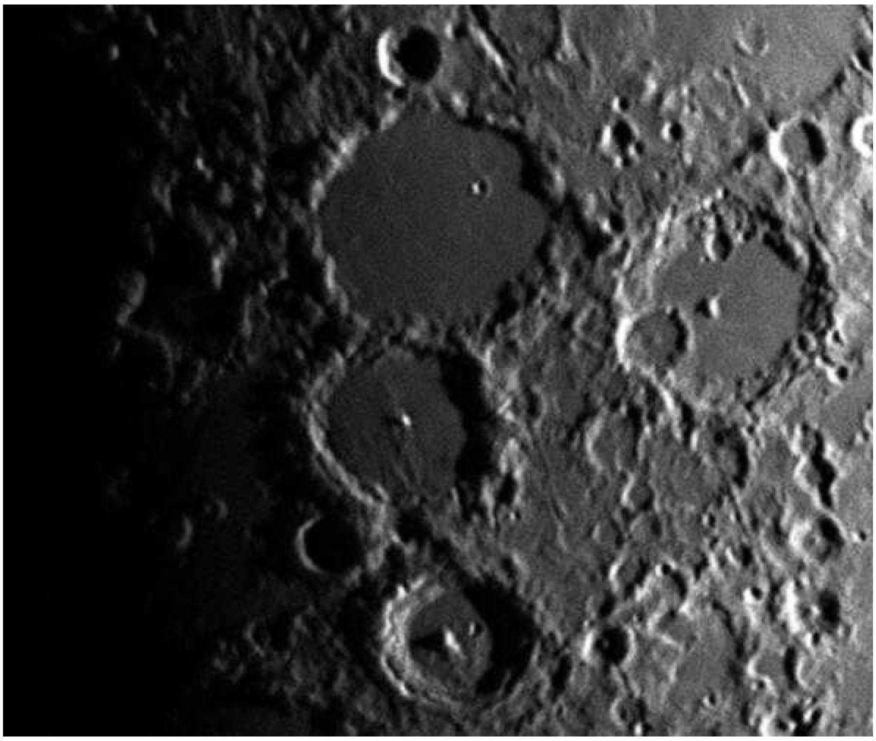

Figure 3. *Alphonsus as imaged by Facundo Gramer (AEA) on 2019 Dec 05 UT 02:22 and orientated with north towards the top.*

As readers may know, Alphonsus is famous for at least three pyroclastic dark spots on the floor. However, it seems that under sunrise conditions they are simply difficult/impossible to see, and there is so much shading on the floor anyway. So therefore, we shall assign a weight of 0 to this report and effectively remove it from the ALPO/BAA TLP database.

Conon: On 2019 Dec 07 UT 03:30 Aylen Borgatello (AEA) imaged this crater under similar illumination, to within ±0.5° to the following report from the 1940s report:

Conon 1941 Feb 07 UT 03:00? Observed by Vaughon (Des Moines, Iowa, 3" reflector) "Faint bright spot on floor, no definite outline (??? reported 6th, but if local time 7th in UT)" NASA catalog weight=3. NASA catalog ID #484. ALPO/BAA weight=1.

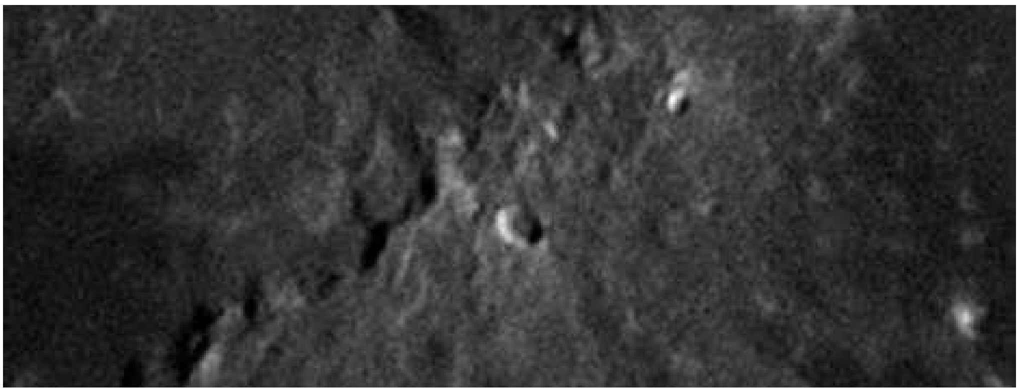

Figure 4. *Conon as imaged by Aylen Borgatello (AEA) on 2019 Dec 07 UT 03:30 and orientated with north towards the top.*

You can quite clearly see in Fig. 4 a faint spot near the centre of Conon. It is just some hilly terrain. I think we can therefore remove this report from the ALPO/BAA TLP database by assigning a weight of 0.

Herodotus: On 2019 Dec 08 UT 19:12 Phil Denyer (BAA) imaged Herodotus midway between similar illumination for two past TLP events – 25 minutes prior to the former observing window and 33 minutes before the opening window of the latter:

Herodotus 1966 Jun 30 UT 03:10-03:35 Observed by Bartlett (Baltimore, MD, USA) described in the NASA catalog as: "Bright pseudo-peak again vis. within floor shadow. Peak est. 5 bright. Had seen it at successive lunations in '66" 4" x280 refractor used. NASA catalog weight=4. NASA catalog TLP ID No. #950. ALPO/BAA weight=3.

On 2017 Sep 02/03 UT 23:55-00:30 A.Anunziato (Parana, Argentina, 105 mm Maksutov Cassegrain, x154, seeing 6/10, some interruption from clouds) observed a light spot SE of the centre of the floor of the crater, which came and went in visibility. There is a light spot here, but what was unusual was that the visibility decreased over time. ALPO/BAA weight=1.

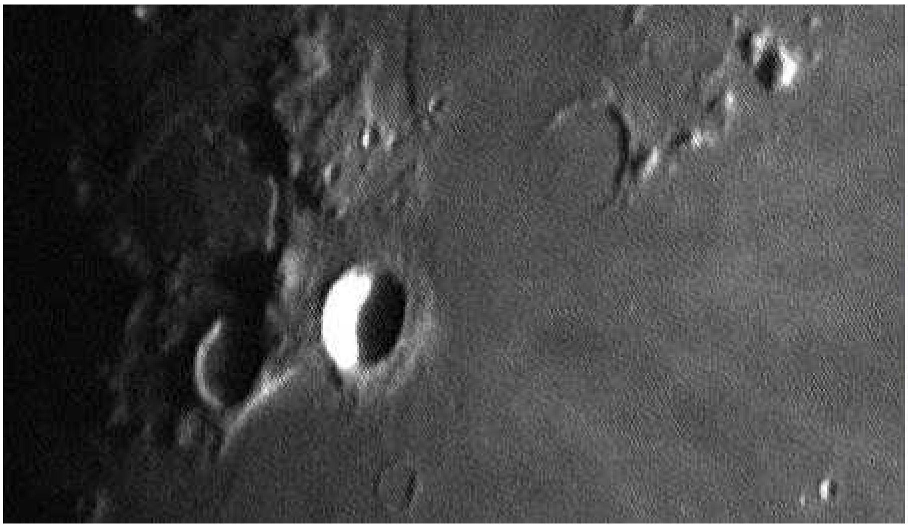

Figure 5. *Herodotus and Aristarchus orientated with north towards the top.* ***(Left)*** *An image by Phil Denyer (BAA) taken on 2019 Dec 18 UT 19:12.* ***(Right)*** *A sketch by Alberto Anunziatio made on 2017 Sep 02/03 UT 23:55-00:30.*

Fig. 5 left shows no sign of the pseudo peak that Bartlett mentions, nor the light spot on the floor that Alberto sketched (Fig. 5 – Right). We shall therefore leave the weights of these two past reports the same.

Sirsalis: On 2019 Dec 09 UT 19:19 Bob Stuart (BAA) imaged and at 19:24-19:32 UT Trevor Smith (BAA) observed this crater under similar illumination (±0.5°) to the following GLR TLP observation:

Sirsalis 1999 Jan 30 UT 01:00-01:20 Observed by Giuseppe Sorrentino (Italy) described as: "A temporary change in appearance to sunlit floor of crater" for further references including images please see: http://digilander.libero.it/gibbidomine/sirsalis.htm *. ALPO/BAA weight=1.*

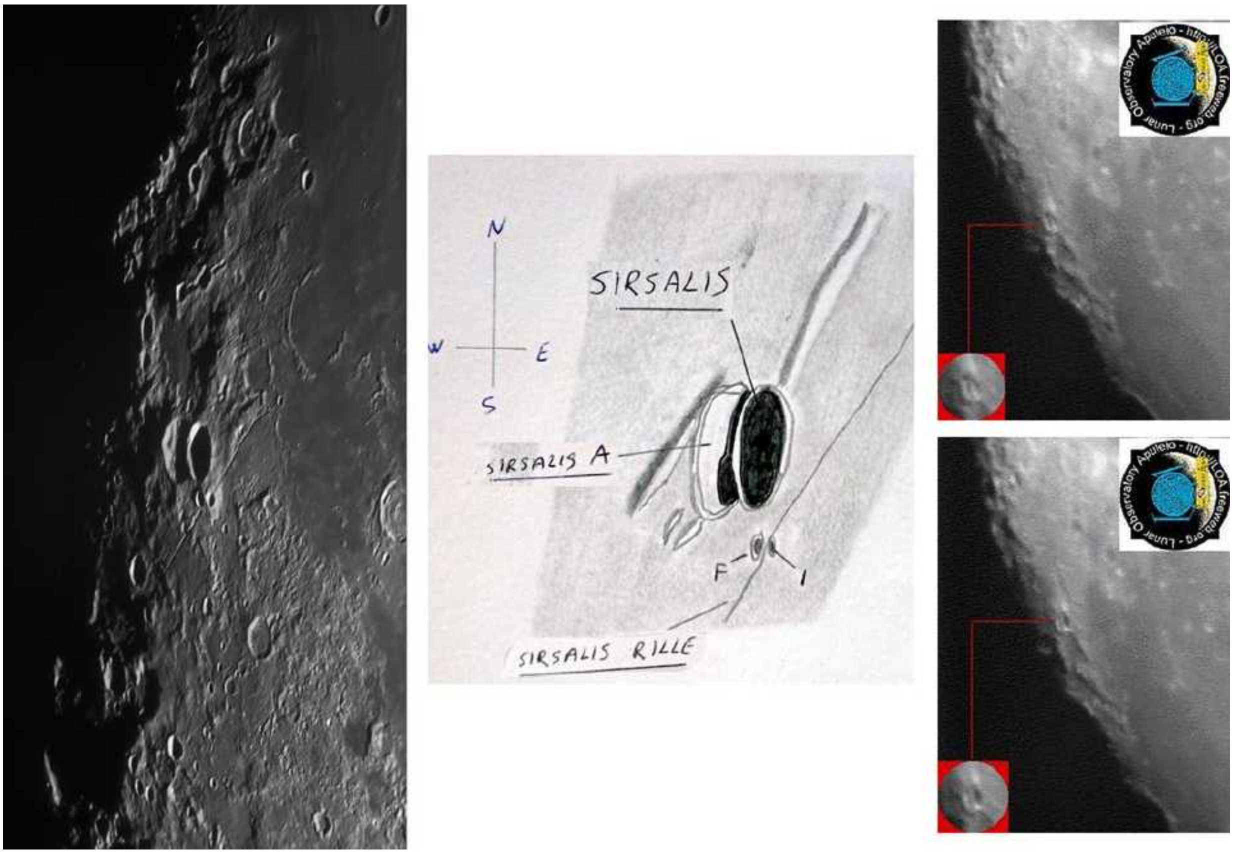

Figure 6. *Sirsalis orientated with north towards the top.* ***(Left)*** *An image by Bob Stuart (BAA) taken on 2019 Dec 09 UT 19:19.* ***(Centre)*** *A sketch by Trevor Smith (BAA) made on 2019 Dec 09 UT 19:24-19:32 – note that the sketch has been re-orientated and the labels switched around to match Bob Stuart's image.* ***(Right)*** *Two images from the GLR web site showering a TLP in Sirsalis from 1999 Jan 30 UT 01:00-01:20, taken by Giuseppe Sorrentino (GLR).*

Although I was not coordinating the TLP sections of ALPO or the BAA at the time, I am familiar with the debate that took place between GLR, UAI, and REA astronomical organisations concerning this event. Although I have not seen all the Sorrentino images (Fig. 6 – Right), based upon Bob's image (Fig. 6 – Left) and Trevor's sketch (Fig. 6 – Centre), as well as the image scale of the GLR images, I think that I would probably come down on the conclusion made by UAI that the effect seen was the result of atmospheric turbulence and a low image scale. If anybody still has all the original images, it would be interesting to run them through a modern-day image stacking program to see if they can give us more information. But for now, I think I will lower the weight to 0 as there is not much more we can do with repeat illumination studies of this crater.

Mons Piton: On 2019 Dec 10 UT 03:01 Alberto Anunziato (AEA) imaged this mountain under similar illumination (to within ±0.5°) to the following report:

On 1982 Aug 02 at UT 22:59-23:10 M.Price (Frimley, Surrey, UK, seeing=II-III) found that the north point of this mountain appeared poorly defined and merged into the surroundings - however suspected that this might be normal for this colongitude? The Cameron 2006 catalog ID=179 and weight=1. The ALPO/BAA weight=1.

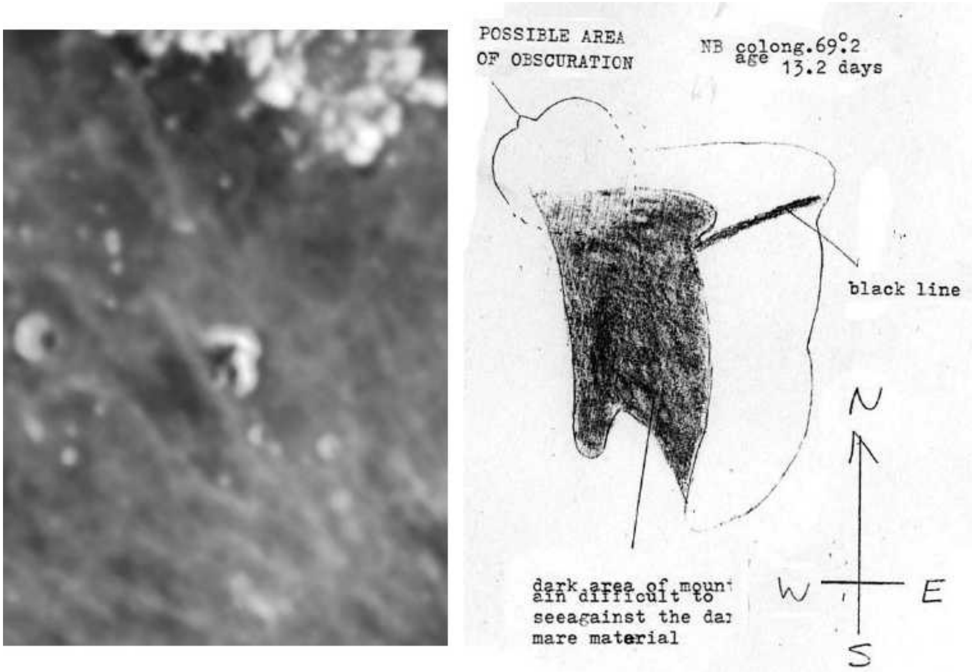

Figure 7. *Mons Piton orientated with north towards the top. (Left) Highly enlarged section of an image submitted by Alberto Anunziato, taken on 2020 Dec 10 UT 01:40.* ***(Right)*** *A sketch by Marcus Price (BAA) made on 1982 Aug 02 UT 22:59-23:10.*

Alberto's image (Fig. 7 – Left) clearly shows a fuzzy area that Price depicted as a candidate obscuration (Fig. 7 – right). I think therefore we can lower the weight to 0 and remove this from the ALPO/BAATLP catalog.

Plato: On 2019 Dec 10 UT 09:41 Maurice Collins (ALPO/BAA/RASNZ) imaged this crater in colour when the illumination was similar to ±0.5°to the following 1960s observation:

Plato 1964 Nov 14 UT 01:00? Observed by Bartlett (Baltimore, MD, USA, 4" refractor?) "Peak on E. wall brilliant white, strong blue band at inner base; on S. wall was a small, bright red spot." NASA catalog weight=4. NASA catalog ID #864. ALPO/BAA weight=3.

Figure 8. *Colour image of Plato taken by Maurice Collins (ALPO/BAA/RASNZ) on 2019 Dec 10 UT 09:41, reoriented with north towards the top. The image has been colour normalized and the colour saturation increased to 60%.*

Fig. 8 shows none of the colour effects that Bartlett described, using his 3" refractor. It could be that they were related to chromatic aberration in the 3" refractor. Unfortunately, it is difficult to find out, so we shall leave the weight at 3 for now as the small red spot that Bartlett describes is unusual and difficult to replicate with standard colour producing mechanisms in our atmosphere, or with optics.

Aristarchus: On 2019 Dec 11 two AEA observers imaged this crater at 04:45 and 05:42 under similar illumination (±0.5°) to the following TLP reports:

On 1980 Aug 25 at UT06:55-07:10 Bartlett (Baltimore, MD, USA, 4.5" reflector, x40-150, seeing=4 and transparency=4) found the west wall bands of Aristarchus to be faint initially and at 07:00 a pale red colour appeared suddenly (and lasted for 2 minutes) on the inner south east wall, and then into south west BS to the west BS. "BS" meaning in Bartlett's notation a bright spot. There was no violet glare this time. Cameron 2006 catalog ID=106 and weight=4. ALPO/BAA weight=3.

Aristarchus 1973 Jun 15 UT 06:12-06:21 Observed by Bartlett (Baltimore, MD, USA, 3" refractor x54, x100, x300, x360, S=3, T=3) "Pinkinsh-red glow on F., wall -- where he usually sees the violet glare. (TLP albedo=7?, normal=5?, nearby plain=1?). All along rim nr. crest & went over EWBS. Wanted to compare a bright spot on Lyell with Aris. wall brightness. At 0612h pink glow changed to a rust-brown, fading rapidly & gone at 0615h. First time he had ever obs. a red glow. (in 20 yrs)."NASA catalog weight=4 (high). NASA catalog ID #1369.

Aristarchus 1969 Apr 01 UT 18:35 Observed by Kozyrev (Crimea, Ukraine, 40" reflector). "Spectrograms of an unusual red spot on W. slope at ?=.405, eta=.680. Spot = 1-2 km in diam. Molecules identified were N2 & C2. Later thru clouds crater was bluer in Corralitos (New Mexico) MB (confirm. of activity at Ariz. ?)." NASA catalog weight=5. NASA catalog ID #1119. ALPO/BAA weight=5.

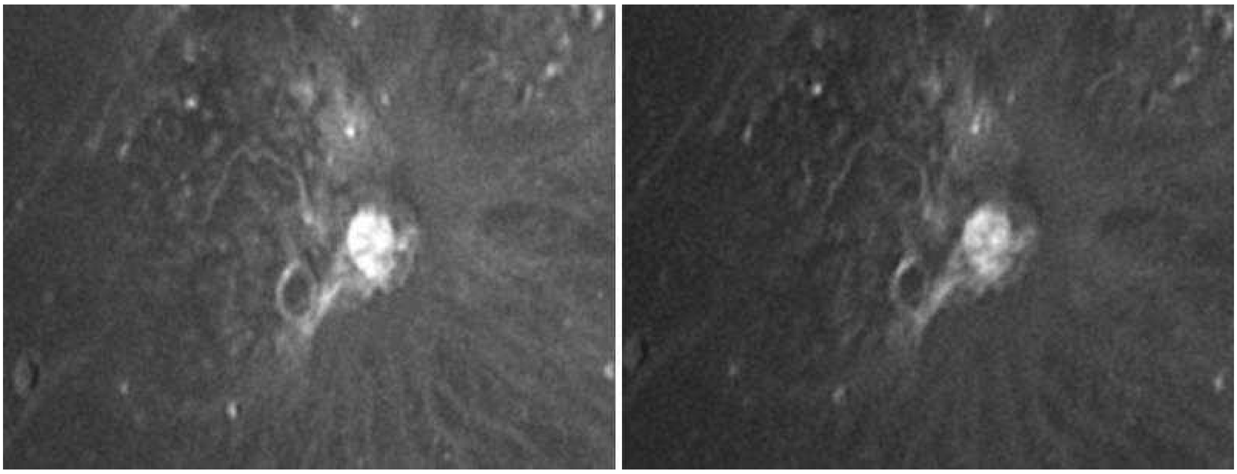

Figure 9. *Aristarchus images captured on 2019 Dec 11 and orientated with north towards the top.* ***(Left)*** *taken by Gabriel Re (AEA) at 04:45UT.* ***(Right)*** *taken by Victoria Gomez (AEA) at 05:42 UT.*

Although the images in Fig. 9 are monochrome, and so won't help to solve the colour/spectral reports in the TLP descriptions above, they do at least illustrate the general routine appearance of the crater as would have been seen by the observers concerned. We shall leave the weights as they are for now.

Plato: On 2019 Dec 15 UT 04:30-04:55 Jay Albert (ALPO) observed visually this crater under similar illumination (±0.5°) to the following report:

On 1984 Nov 11 at UT21:00? Marshall (England) noted that there was no normal brightness on the floor to most southernmost craterlet. The Cameron 2006 catalog ID=253 and the weight=2. The ALPO/BAA weight=1.

Jay found that Plato's east wall was very bright and that the central craterlet, N pair and S craterlet were all seen. The entire floor was darker than Mare Frigoris and Mare Imbrium. However, unlike the TLP description, the floor actually appeared slightly brighter in an ill-defined E-W strip near the southern craterlet. I also cannot find this report in the ALPO/BAA archives. We shall therefore leave the report at a weight of 1.

Aristarchus: On 2019 Dec 17 UT 05:09 Walter Elias imaged the Moon in colour and captured the Aristrachus area under similar illumination, to within (±0.5°, to the following report:

In 1964 Jan 05 at UT 22:00? Doherty (Stoke-on-Trent, UK, 3" refractor, 8" or 10" reflector) observed Aristarchus to be purplish-blue in colour. The Cameron 1978 catalog ID=794 and weight=3. The ALPO/BAA weight=3.

Figure 10. *A colour image of the NW of the Moon, taken by Walter Elias on 2019 Dec 17 UT 95:09, showing Aristrachus. The supplied image has been high passed filter and its colour saturation increased before it was submitted to the Lunar Section. The purple loop around Aristrachus is a processing artefact.*

Although Fig. 10 has been sharpened a little heavily as can be seen by the bright ring on the limb of the Moon, we can at least see some blueness to Aristarchus crater, though the purple line is probably an artefact of then image processing. I am tempted though to lower the weight from 3 to 2 due to the craters colour having at least some similarity to the original report.

General Information: For repeat illumination (and a few repeat libration) observations for the coming month - these can be found on the following web site: http://users.aber.ac.uk/atc/lunar_schedule.htm . Only by re-observing and submitting your observations can we fully resolve past observational puzzles. To keep yourself busy on cloudy nights, why not try 'Spot the Difference' between spacecraft imagery taken on different dates? This can be found on: http://users.aber.ac.uk/atc/tlp/spot_the_difference.htm . If in the unlikely event you do ever see a TLP, firstly read the TLP checklist on http://users.aber.ac.uk/atc/alpo/ltp.htm , and if this does not explain what you are seeing, please give me a call on my cell phone: +44 (0)798 505 5681 and I will alert other observers. Note when telephoning from outside the UK you must not use the (0). When phoning from within the UK please do not use the +44! Twitter TLP alerts can be accessed on https://twitter.com/lunarnaut .

Dr Anthony Cook, Department of Physics, Aberystwyth University, Penglais, Aberystwyth, Ceredigion, SY23 3BZ, WALES, UNITED KINGDOM. Email: atc @ aber.ac.uk

BAA LUNAR SECTION CONTACTS

Director and Circulars Editor
Bill Leatherbarrow (w.leatherbarrow1 @ btinternet.com)

Assistant Director
Tony Cook (Coordinator,
Lunar Change project) (atc @ aber.ac.uk)

Website Manager
Stuart Morris [contact link via the Section website at https://britastro.org/section_front/16]

Committee members
Tim Haymes (Coordinator,
Lunar Occultations) (occultations @ stargazer.me.uk)
Robert Garfinkle (Historical) (ragarf @ earthlink.net)
Raffaello Lena (Coordinator,
Lunar Domes project) raffaello.lena59 @ gmail.com
Nigel Longshaw
Barry Fitz-Gerald